Sex-specific divergent maturational trajectories in the postnatal rat basolateral amygdala

Pauline Guily [1,2], Olivier Lassalle[1,2], Olivier JJ Manzoni[1,2]

1 INMED, INSERM, Aix Marseille Univ, France.
2 Cannalab Cannabinoids Neuroscience Research International Associated Laboratory. INSERM-Aix-Marseille University/Indiana University.

Corresponding author:
Olivier Manzoni, PhD.
INMED, INSERM U901,
Parc Scientifique de Luminy,
BP13 – 13273 Marseille cedex 09, France.
Email : olivier.manzoni@inserm.fr

Abstract: 332 words
Main text: 5989 words
Figures: 9
Supplementary figure: 1
Tables: 16

Abstract
The basolateral amygdala (BLA), the part of the amygdala complex involved in the transduction of perceptual stimuli into emotion, undergoes profound reorganization at adolescence in rodents and humans. How cellular and synaptic plasticity evolve throughout postnatal development in both sexes is only partially understood. We used a cross-sectional approach to compare the morphology, neuronal, and synaptic properties of BLA neurons in rats of both sexes at adolescence and adulthood. While BLA pyramidal neurons from rats of both sexes displayed similar current-voltage relationships, rheobases, and resting potentials during pubescence, differences in these parameters emerged between sexes at adulthood: BLA neurons were more excitable in males than females. During pubescence, BLA neuron excitability was highest in females and unchanged in males; male action potentials were smaller and shorter than females and fast afterhyperpolarizations were larger in males. During post-natal maturation, no difference in spine density was observed between groups or sexes but spine length increased and decreased in females and males, respectively. A reduction in spine head diameter and volume was observed exclusively in females. Basic synaptic properties also displayed sex-specific maturational differences. Stimulus-response relationships and maximal fEPSP amplitudes where higher in male adolescents compared with adults but were similar in females of both ages. Spontaneous excitatory postsynaptic currents mediated by AMPA receptors were smaller in BLA neurons from adolescent female compared with their adult counterparts but were unchanged in males. These differences did not directly convert into changes in overall synaptic strength estimated from the AMPA/NMDA ratio, which was smaller in adolescent females. Finally, the developmental courses of long-term potentiation and depression (LTP, LTD) were sexually dimorphic. LTP was similarly present during the adolescent period in males and females but was not apparent at adulthood in females. In contrast, LTD followed an opposite development: present in adolescent females and expressed in both sexes at adulthood. These data reveal divergent maturational trajectories in the BLA of male and female rats and suggest cellular substrates to the BLA linked sex-specific behaviors at adolescence and adulthood.

Introduction

The basolateral amygdala (BLA), a limbic area massively connected to cortical and sub cortical structures is at the interface of perception, emotion, and motor behaviors. Its role in the processing of fearful and rewarding stimuli, as well as emotional memory, is now well established (Bocchio et al., 2017; Janak & Tye, 2015; Phelps, 2004). A growing body of evidence indicates sex-differences in these functions (Cahill et al., 2004; Canli et al., 2002; Greiner et al., 2019; Gruene et al., 2015; Lebron-Milad & Milad, 2012). Moreover, the BLA is implicated in the etiology of neuropsychiatric diseases including post-traumatic stress disorder, depression, and anxiety (Daviu et al., 2019; Mahan & Ressler, 2012; Nestler et al., 2002), characterized by their higher prevalence in the female population (Christiansen & Berke, 2020; Kuehner, 2017; McLean et al., 2011). While the study of females' brains and sex-differences in preclinical research have recently gained momentum (Shansky & Murphy, 2021), sex-differences in the functions of the BLA have mostly been studied in pathological rodent models (Blume et al., 2019; Geary et al., 2021; Guadagno et al., 2020; Przybysz et al., 2021) and the physiological development of the female BLA remains partially understood.

At adolescence, neural networks are rearranged to allow the emergence of novel behaviors and the following transition to adult-specific circuits (Casey et al., 2008; Spear, 2000). Puberty is a particular time window of adolescent neurodevelopment, characterized by the arrival of sexual maturity and accompanied by a profound regulation of sex hormones (Schneider, 2013). Both adolescence and puberty are essential periods of postnatal brain maturation and are characterized by heightened susceptibility to mental disorders (Schneider, 2013). Specifically, changes in puberty onset are associated with increased risk for depression, mostly in girls (Graber, 2013; Patton et al., 2008). Studies also suggest that sex-differences in depression prevalence emerge, or at least strengthen, during adolescence (Breslau et al., 2017). Additionally, there is consistent evidence indicating that the BLA activity is not mature at adolescence in humans (Scherf et al., 2013), and that puberty influences the maturation of the human amygdala (Bramen et al., 2011; Goddings et al., 2014). However, the magnitude of amygdala reorganization and possible sex differences during this period remain to be fully explored.

In adult rats, sex and estrus differences in excitatory and inhibitory inputs, as well as in the spine density of principal neurons residing in the lateral nucleus (LA) and the basal nucleus (BA) of the BLA have been reported (Blume et al., 2017). Long-term potentiation (LTP) of LA-BA synapses in both male and female juvenile rats has been described (Bender et al., 2017; Guadagno et al., 2020). LTP and long-term depression (LTD) are both sensitive to sexual hormones in the BLA (Bender et al., 2017; Krężel et al., 2001; Yang et al., 2017), but little is known about sex-specific maturational trajectories of synaptic plasticity between puberty and adulthood. To our knowledge, no study to date has compared neuronal and synaptic properties in the BLA during the pubertal period in both sexes. To address this gap in knowledge, we compared neuronal properties and excitatory transmission in the BLA of pubescent and adult rats of both sexes. Using ex-vivo electrophysiological recordings in rat BLA slices, we report that excitatory neurons undergo complex sex-specific maturational sequence development. Some parameters such as intrinsic properties and action potential properties of neurons exhibit sex-differences only at a specific time of development, whereas other parameters such as basic excitatory transmission and synaptic plasticity display different maturational profiles between male and female rats.

Material and methods

Further information and requests for resources should be directed to the Lead Contact, Olivier J.J. Manzoni (olivier.manzoni@inserm.fr).

Animals

Animals were treated in compliance with the European Communities Council Directive (86/609/EEC) and the United States NIH Guide for the Care and Use of Laboratory Animals. The French Ethical committee authorized the project APAFIS#26537-2020070812023339. All rats were obtained from Janvier Labs and group-housed (two to four rats per cage) with ad libitum access to food and water. All groups represent data from a minimum of 2 litters. The animal housing room was maintained on a 12 h-day light/dark cycle at constant room temperature (20 ± 1°C) and humidity (60%). Data were collected blind to the estrous cycle unless specified. Female and male rats were classified based on the timing of their pubertal maturation. Male and female rats do not reach puberty at the same time (Schneider, 2013). Thus, the female ages groups were Pubescent 33<P<38 and Adult at 90<P<120. Male groups were: Pubescent 41<P<56 and Adult at 90<P<120 (Supplementary Fig. 1A). All animals were experimentally naïve and used only once.

Electrophysiology

Male and female rats were anesthetized with isoflurane and killed as previously described (Bara et al., 2018; Borsoi et al., 2019; Scheyer et al., 2019, 2020a, 2020b). The brain was sliced (300 µm) in the coronal plane with a vibratome (Integraslice, Campden Instruments) in a sucrose-based solution at 4°C (in mM as follows: 87 NaCl, 75 sucrose, 25 glucose, 2.5 KCl, 4 $MgCl_2$, 0.5 $CaCl_2$, 23 $NaHCO_3$ and 1.25 NaH_2PO_4). Immediately after cutting, slices containing the basolateral amygdala (BLA) were stored for 1h at 32°C in a low-calcium ACSF that contained (in mm) as follows: 130 NaCl, 11 glucose, 2.5 KCl, 2.4 $MgCl_2$, 1.2 $CaCl_2$, 23 $NaHCO_3$, 1.2 NaH_2PO_4, and were equilibrated with 95% O_2/5% CO_2 and then held at room temperature until the time of recording.

During the recording, slices were placed in the recording chamber and superfused at 2 ml/min with normal ACSF that contained (in mm): 130 NaCl, 11 glucose, 2.5 KCl, 2.4 $MgCl_2$, 2.4 $CaCl_2$, 23 $NaHCO_3$, 1.2 NaH_2PO_4, equilibrated with 95% O_2/5% CO_2. All experiments were done at 32°C. The superfusion medium contained picrotoxin (100 µM, Sigma) to block GABA-A receptors, except for low frequency stimulation (LFS) experiments. All drugs were added at the final concentration to the superfusion medium. Field and whole-cell patch-clamp recordings were performed with an Axopatch-200B amplifier, data were low pass filtered at 2kHz, digitized (10 kHz, DigiData 1440A, Axon Instrument), collected using Clampex 10.2 and analyzed using Clampfit 10.2 (all from Molecular Device, Sunnyvale, USA).

Whole-cell patch-clamp of visualized BLA principal neurons and field potential recordings were made as previously described (Bara et al., 2018; Borsoi et al., 2019; Scheyer et al., 2019, 2020a, 2020b) in coronal slices containing the BLA. Neurons were visualized using an upright microscope with infrared illumination. The intracellular solution was based on K^+ gluconate (in mM: 145 K^+ gluconate, 3 NaCl, 1 $MgCl_2$, 1 EGTA, 0.3 $CaCl_2$, 2 Na^{2+} ATP, and 0.3 Na^+ GTP, 0.2 cAMP, buffered with 10 HEPES). The pH was adjusted to 7.2 and osmolarity to 290 – 300 mOsm. Electrode resistance was 2 – 4 MOhms. Access resistance compensation was not used, and acceptable access resistance was <30 MOhms. The potential reference of the amplifier was adjusted to zero prior to breaking into the cell. Current-voltage (I-V) curves were made by a series of hyperpolarizing to depolarizing 50 pA current steps after breaking into the cell. To determine rheobase and action potential properties a series of depolarizing 10 pA current steps was applied. Membrane resistance was estimated from the I–V curve around resting membrane potential (Bara et al., 2018; Borsoi et al., 2019; Scheyer et al., 2019, 2020a, 2020b).

Spontaneous EPSCs (sEPSCs) were recorded at -70mV for at least 10 min as previously described (Kasanetz & Manzoni, 2009; Martin et al., 2016). To determine AMPA/NMDA ratios, the intracellular solution was based on cesium methanesulfonate (Cs^+Meth, mM): 143 $CsMeSO_3$, 5 NaCl, 1 $MgCl_2$, 1 EGTA, 0.3 $CaCl_2$, 10 HEPES, 2 Na_2ATP, 0.3 NaGTP and 0.2 cAMP (pH 7.3 and 290-300 mOsm). AMPA/NMDA ratios were calculated by measuring evoked EPSCs (having AMPAR and NMDAR components) at +30 mV. The AMPAR component was isolated by bath application of an NMDAR antagonist (APV; 50 μM, Tocris)(Kasanetz & Manzoni, 2009).
For extracellular field potential recordings, the stimulating electrode was positioned in the lateral amygdala (LA), close to the external capsula (EC), dorsolateral to the recording electrode placed into the adjacent BA (Supplementary Fig. 1B). The glutamatergic nature of the field EPSP (fEPSP) was systematically confirmed at the end of the experiments using the ionotropic glutamate receptor antagonist CNQX (20 μM), which specifically blocked the synaptic component without altering the non-synaptic component. Both fEPSP area and amplitude were analyzed. Stimulation was performed with a glass electrode filled with ACSF and the stimulus intensity was adjusted ~60% of maximal intensity after performing an input–output curve. For LTP experiments, baseline stimulation frequency was set at 0.1 Hz and plasticity was induced by a theta burst stimulation (TBS; 5 trains of 4 pulses at 100 Hz, 200 ms train interval, repeated 4 times at 10 s interval). For LTD experiments, baseline stimulation frequency was set at 0.0666 Hz and plasticity was induced by low frequency stimulation (LFS; 900 pulses at 1 Hz).

Analysis

Action potential properties were determined from the first spike induced during current clamp experiment. The voltage at which point the dV/dt trace first passed 5 mV/ms was the threshold. fAHP was measured at a local minimum directly following spike's repolarization within a couple of ms. The mAHP was measured at a local minimum distinct from the fAHP and occurring 15-150 ms after the spike. The frequency and amplitude of sEPSCs were analyzed with Axograph X using a double exponential template: f(t) = exp(-t/rise) + exp(-t/decay) (rise = 0.5 ms and decay = 3 ms). The detection threshold for the events was set at 2.5 times the baseline noise SD. For AMPA/NMDA ratios, NMDAR component was obtained by digital subtraction of the AMPA-EPSC from the dual component EPSC (AMPA/NMDA ratio = peak AMPA-EPSC at +30mV/ peak NMDA-EPSC at +30 mV). For field recording experiments, the magnitude of plasticity was calculated at 30–40 min after induction as percentage of baseline responses.

Dendritic spines' reconstruction and quantification

All neurons recorded with Cs^+Meth solution were also loaded with neurobiotin through patch pipettes. Slices were then fixed overnight in 4% paraformaldehyde, rinsed with PBS and incubated overnight at 4°C with streptavidin-AlexaFluor555 (1:200 in PBS). Slices were mounted for subsequent confocal imaging. All filled neurons corresponded to typical glutamatergic BLA neurons (Washburn & Moises, 1992) (e.g, large cell body, spiny dendrites, pyramidal to stellate shape). Only neurons showing proper filling of the dendritic tree were included in the analysis. Five to eleven dendrites per neuron were analyzed. Dendrites were located approximatively at 70 to 140 μm of the soma. Stack images were acquired using a Zeiss LSM-800 confocal microscope equipped with a 40 oil-immersion objective (NA: 1,4). Frame size was of 512x512 pixels with a x4 zoom. Laser power and photomultiplier gain were adjusted to obtain few pixels with maximum intensity on dendrite shaft and the offset range was tuned to cutoff background noise. Tri-dimensional deconvolution of each stack was performed with Fiji software to compensate the spherical aberration and to correct the z-

smear for reliable spine morphology. Point-spread function (PSF) were computed using PSFGenerator plugging (Kirshner et al., 2013) and deconvolution was realized with DeconvolutionLab2 plugin (Sage et al., 2017) using the Richardson-Lucy method. Tri-dimensional reconstruction and semiautomated analysis were performed with Imaris (Bitplane, Zurich, Switzerland).

Statistics

Statistical analysis of data was performed with Prism (GraphPad Software) using tests indicated in the main text after outlier subtraction (Grubb's test, alpha level 0.05). All values are given as mean ±SEM, and statistical significance was set at $p<0.05$.

Results

The aim of this study was two-fold. First, we aimed to uncover potential sex-differences at two key moments of development (pubescence and adulthood), and second, we compared maturational trajectories according to sex. Experiments were done in rats of both sexes at pubescent (female 33<P<38; male 41<P<56) and adult stages (at 90<P<120 for both sexes). For the sake of clarity, we chose to present each studied parameter in a way that appropriately highlighted either sex-differences or maturational differences. All complementary statistics can be found in Tables 1-16.

Sex-specific differences in intrinsic properties of rat BLA principal neurons emerge in adulthood.

Within the BLA, LA and BA principal neurons have distinct neuronal and synaptic properties (Blume et al., 2017). Thus, we purposedly restrained this study to only one of these nuclei and chose the BA. Intrinsic properties are essential features of pyramidal neurons as well as key determinants of synaptic and network properties (Debanne & Poo, 2010). To compare intrinsic firing properties of principal neurons in our experimental groups, we performed patch-clamp recordings of BLA neurons in acute BLA slices obtained from pubescent and adult male or female rats and measured the membrane reaction profiles in response to a series of somatic current steps (Fig. 1, Tab. 1-2). All recording sites are reported in Supplementary figure 1.

At pubescence, all recorded BLA pyramidal neurons showed similar and superimposable I–V plots independent of sex (Fig. 1A). Similarly, the resting membrane potential (Fig. 1B), the rheobase (Fig. 1C), and the number of depolarization-driven spikes (Fig. 1D) were similar within and between sex groups.

At adulthood however, differences emerged between sexes: there was significant, albeit small, shift between I–V plots of males and females (Fig. 1E). Additionally, the resting membrane potential (Fig. 1F) and the rheobase (Fig. 1G) of BLA pyramidal neurons significantly differed between sexes. Furthermore, as estimated from the number of depolarization-driven spikes, adult males showed more action potentials in response to somatic current steps, compared with females (Fig. 1H).

Together these data show that sex-specific differences in intrinsic properties emerge at adulthood in BLA pyramidal neurons and that male BLA neurons display a higher excitability than female neurons at the same age.

Action potentials in BLA principal neurons diverge at pubescence

Changes in spike trains and excitability could partly be explained by changes in ion channel conductance which generate the different phases of action potentials (Hunsberger & Mynlieff, 2020; Matos et al., 2020; Y. Zhang et al., 2020). To gain insight into this matter, we next explored waveform properties of individual action potentials (Fig. 2, Tab. 3-4). Action potential threshold did not vary between our four groups (Fig.2B), but sex-differences in other action potential properties were found in pubescent rats. Thus, at pubescence, action potentials' amplitude (Fig. 2C) and half-width (Fig. 2D) were larger in females compared with males. Specifically, the decay time (Fig. 2F) was slower in female BLA neurons while rise times were not different (Fig. 2E), supporting the existence of sex-differences in the repolarization phase of pubescent rat.

At adulthood, action potentials of BLA principal neurons displayed similar amplitude (Fig. 2C), half-width (Fig. 2D), rise times (Fig. 2E) and decay times (Fig. 2F).

Rather counter intuitively, these data suggest that, in contrast to sex-differences in other intrinsic properties, sex-differences in action potential properties are only found at pubescence and disappear in adulthood in BLA principal neurons.

The prolonged activation of calcium-dependent potassium channels (KCa) during the repolarization phase of action potentials leads to an afterhyperpolarization (AHP) potential below the action potential threshold. The medium AHP (mAHP, Fig. 3A), is tightly linked to neuronal excitability and sensitive to stress exposure in the BLA (Faber et al., 2001; Hetzel & Rosenkranz, 2014; Rau et al., 2015). Less is known about the fast AHP (fAHP, Fig. 3A), however, it undergoes a profound maturation within the first post-natal month in the BLA (Ehrlich et al., 2012). The amplitudes of the fAHP and mAHP were measured in the first action potential recorded at the rheobase (Fig. 3, Tab. 5-6).

In every group, a large majority of neurons displayed a fAHP (Fig. 3C). In pubescent animals, the fAHP amplitude was significantly greater in males compared with females. This sex-difference was no longer present in adults (Fig 3D). No significant maturation of the fAHP was found in either male or female rats. Conversely, we did not record sex-differences in the mAHP amplitude of age-matched animals, however, there was a maturation of the mAHP, illustrated by a larger mAHP in adult females compared with pubescent males and females (Fig. 3E).

Synaptic properties in the BLA of pubescent and adult rats

Synaptic properties were compared and input–output curves constructed from the fEPSP amplitude vs increasing stimulation intensities at the BLA from brain slices of our 4 groups (Fig. 4, Tab. 7-8). Significant differences in stimulus-response relationship and maximal fEPSP amplitude were found between pubescent and adult males (Fig. 4B, 4D). In females, the stimulus-response relationship did significantly vary between pubescents and adults (Fig. 4A), however the maximal fEPSP amplitudes did not (Fig. 4C), despite a propensity towards larger fEPSP in pubescent females.

At excitatory synapses, the relative levels of AMPAR and NMDAR is a measure of synaptic integration and plasticity (Malinow & Malenka, 2002). We compared the ratio between AMPAR- and NMDAR-evoked EPSCs (AMPA/NMDA ratio) in adolescent and adult BLA neurons from rats of both sexes (Fig. 5, Tab. 9-10). This parameter significantly varied between males and females at pubescence (Fig. 5A), males having a greater AMPA/NMDA ratio. In BLA slices of pubescent males, the distribution of data clearly shed light on two subgroups of neurons: one group displayed AMPA/NMDA ratio like females and the other exhibited AMPA/NMDA ratios higher than females (Fig 5C). In adult rats, the AMPA/NMDA ratio was similar across sexes (Fig. 5B, 5D).

To extend our portrait of excitatory BLA synapses, AMPAR spontaneous EPSCs (sEPSCs) were isolated in BLA neurons voltage-clamped at -70 mV (Fig. 6, Tab. 11-12). Whereas the frequency of AMPAR sEPSCs remained invariable in females (Fig. 6B), the amplitude of AMPAR sEPSCs was less in BLA neurons recorded from pubescent females compared with their adult counterparts (Fig. 6C) and the distribution of sEPSC amplitudes was shifted toward lower values in adolescent female rats (Fig. 6D). In contrast, both AMPA sEPSCs amplitude and frequency remained invariable in male littermates (Fig. 6E-H).

Sex specific maturation of BLA neurons dendritic spines

Dendrites of BLA principal neurons are characterized by the presence of numerous spines which are the main contact of glutamatergic inputs (Brinley-Reed et al., 1995; Farb et al., 1992; Radley et al., 2007; Washburn & Moises, 1992). These spines are subject to intense maturational processes in the postnatal brain (Moyer & Zuo, 2018) and the BLA (Bosch & Ehrlich, 2015). Moreover, sex-differences in spine density have also been reported in the adult

BLA (Blume et al., 2017). Thus, to elucidate the sex-specific maturation of excitatory synapses in BLA principal neurons, we performed an ex vivo three-dimensional reconstruction three-dimensional reconstruction of neurobiotin-filled BLA neurons (Fig. 7, Tab. 13-14).

Quantitative analysis of dendritic spine density and architecture revealed no change in the density of spines in our different groups (Fig. 7A-B; all classes of spines were analyzed). Analyzing the cumulative distribution of spine length, spine head diameter, and spine volume, we found significant differences between adult and pubescent spines of sex-matched animals (Fig. 7C-H). Analyzing the total population of spines revealed a more pronounced maturation in females than males. Specifically, there was an augmentation in spine length (Fig. 7C), paralleled by a reduction in spine head diameter (Fig. 7E) and spine volume (Fig. 7G) in adult females compared with pubescents. In males, differences were restricted to a reduction in the spine length of adults compared with pubescent rats (Fig. 7D).

Theta-burst long-term potentiation follows a sex-specific maturational sequence in the rat BLA.

Long-term potentiation (LTP) of excitatory synapses has been extensively studied in the BLA due to its role in fear learning and memory (Pape & Pare, 2010). While most studies measured LTP at sensory inputs onto the LA, LTP at LA-BA synapses has also been reported in male and female rats at young ages (Bender et al., 2017; Guadagno et al., 2020). We elected to investigate LA-BA LTP in the BLA of male and female rats at our two age periods to test the hypothesis of a sexual dimorphism of BLA plasticity. We chose a mild induction protocol (theta burst stimulation, TBS) that allows detecting of altered LTP in rodent models of neuropsychiatric disorders (Iafrati et al., 2016; Labouesse et al., 2017; Manduca et al., 2017; Thomazeau et al., 2014). The LTP-induction protocol was applied to acute BLA slices obtained from our various rat groups during simultaneous recording of extracellular field EPSPs (Fig. 8, Tab. 15).

In female BLA, while the TBS protocol effectively induced a lasting synaptic potentiation in slices obtained from pubescent rats, LTP was not induced by this protocol in slices prepared from adult rats (Fig. 8 A, C, E). In contrast, TBS-LTP was consistently expressed in both pubescent and adult rats (Fig. 8 B, D), albeit to a lesser level at the adult stage compared to adolescent counterpart. Indeed, when plotting the cumulative distribution of LTP percent, data distribution of adults was left shifted compared to pubescent rats, therefor indicating a reduction of TBS-LTP at adulthood (Fig. 8F).

Long-term depression appears at adulthood in the BLA of male rats.

Long-term depression (LTD) is a widespread form of synaptic plasticity (Malenka & Bear, 2004) also present in the rat BLA. Indeed, low frequency stimulation (1hz for 15 min, LFS) at LA-BA synapses reliably induces LTD (S.-J. Wang & Gean, 1999). Thus, we systematically compared LFS-LTD in the BLA of pubescent and adult rats of both sexes (Fig. 9, Tab. 16). A 15-minute, 1Hz stimulation in BLA slices obtained from females in both age groups induces a robust LTD (Fig. 9 A, C, E). This protocol likewise elicited LTD in slices obtained from adult males (Fig. 9 B, D, F). To our surprise, LFS-LTD could not be induced in response to this protocol in pubescent males (Fig. 9 B, D, F). Taken together, the results suggest a degree of sex specificity to the maturational profile of LFS-LTD and TBS-LTP.

Discussion

Cross-sectional portrayal of the morphology and neuronal properties of BLA neurons in rats of both sexes revealed sex-differences specific to adolescence and adulthood.

Sex-differences in intrinsic properties of BLA neurons emerge at adulthood.

We found that adult females had a higher rheobase, hyperpolarized membrane potential, and a lower propensity to trigger action potentials in response to depolarizing current steps than adult males. Consequently, principal neurons in the BLA of adult females are less excitable than those of adult males. Sex-differences in intrinsic properties of adult rats have already been described in other brain regions. Within the medial amygdala, a class of neurons exhibits lower spike frequency in response to depolarizing current in females than in males (Dalpian et al., 2019). In the NAc core, medium spiny neurons are also less excitable in females (i.e. higher rheobase and a hyperpolarized resting potential) than in males (Proaño et al., 2018). In gonadectomized animals these sex-differences were abolished but recapitulated by estradiol (Proaño & Meitzen, 2020). Altogether, these results constitute converging evidence towards less excitable neurons in adult females. The observation that sex differences are not visible at puberty at a time when the estrous cycle of females is not well established supports the instrumental role of gonadal hormones. Stress exposure induces sex-divergent effects in the amygdala: BA neurons' firing rate augments in males and decreases in females (Blume et al., 2019). These changes have been attributed to stress-induced imbalance in excitation and inhibition (Blume et al., 2019; Mozhui et al., 2010; Rosenkranz et al., 2010; W. Zhang & Rosenkranz, 2012), and our results further suggest that initial sex-differences in neuronal intrinsic excitability could participate in the divergent effect of stress seen in males and females.

Sex-differences in action potentials emerge at pubescence

Pubescent males had shorter action potentials with faster repolarization compared with females. An early study reported that sex does not influence the maturation of action potential waveform during the first post-natal month (Ehrlich et al., 2012). However, Guadagno and collaborators observed that juvenile (PND22-PND29) males have shorter action potentials with slower depolarization rates compared with females (Guadagno et al., 2020). Here, we found sex-differences reminiscent of those of pubescence (males still have shorter action potentials but faster repolarization). The current finding that the sex-differences disappear in adults suggests a profound sex-specific maturation of action potentials from prepuberty through late adolescence.

Pubescent females displayed smaller fAHP compared with males. Changes in the expression of large conductance KCa (BKCa) may explain these dissimilarities (Sah & Louise Faber, 2002). In the LA, specific blockade of BKCa leads to smaller fAHPs and slower depolarizations of action potentials. Furthermore, stress exposure recapitulates these effects and is associated with a down-regulation of BKCa channels (Guo et al., 2012). Hence, a down-regulation of BKCa channels in pubescent females compared with males could participate in sex-differences in fAHP but also in depolarization.

Unlike fAHP, mAHP amplitude was not influenced by sex. However, age did influence the mAHP, with larger mAHPs in adult females compared with pubescents. The mAHP results from the activation of apamine-sensitive small conductance KCa channels (Sah & Louise Faber, 2002). Our results are therefore consistent with that idea of sex-specific profiles of SK channels expression during maturation.

Mixed evidence implicate the mAHP in the modulation of intrinsic spiking frequency in BLA neurons (Chen & Lang, 2003; Faber & Sah, 2002; Power & Sah, 2008). Although multiple factors could explain these discrepancies (the age of animals, in vivo vs in vitro, recording in LA or BA), smaller mAHP are consistently linked to an increased excitability. Furthermore, adolescent male rats that are responsive to restraint stress express higher spike frequency in both LA and BA neurons (Hetzel & Rosenkranz, 2014). While this increased excitability is accompanied by smaller mAHP in the LA, there was no effect on the mAHP in BA neurons. Thus, the mAHP is not constantly correlated with the spiking frequency in the BA. When we recorded BA neurons, the increased excitability seen in male adults compared females of the same age was not echoed by sex-differences in the mAHP. Nevertheless, in pubescent, high spiking frequency and smaller mAHP were concomitant (Table 1).

Basic excitatory synaptic properties

We recently showed that the input-profile and the release probability of excitatory synapses to prefrontal cortex (PFC) pyramidal neurons were consistent between pubescence and adulthood in both sexes (Bernabeu et al., 2020). In the BLA, the input-output curves built in pubescent rats reached higher maxima than in adults, in support of the idea that the BLA reaches maturity late in life. Pre-synaptic (e.g. release probability) or post-synaptic (e.g. receptor trafficking, AMPAR and NMDAR expression; Hwang & Lupica, 2020). maturation of the LA-BA synapses could explain the dissimilarities between pubescent and adult rats. In the present study, the AMPA/NMDA ratio in females was stable through development, and thus this mechanism is unlikely to account for the maturation of the input-profile in female rats. The AMPA/NMDA ratio of pubescent males was higher compared with females of the same age and this sex-difference was not found in adults. Interestingly, the distribution of AMPA/NMDA ratios was bi-modal in pubescent but not adult males, perhaps an indication of a specific developmental signature in males. In contrast, previous work from our group conducted in the mice PFC demonstrated that AMPA/NMDA ratios remained stable between adolescence and adulthood (Iafrati et al., 2016). In the NAc (Kasanetz & Manzoni, 2009), AMPA/NMDA ratios are homogenous in adolescent mice while they express a bi-modal distribution in adults, contrary to what we observed in the BLA. Unfortunately, the aforementioned studies did not include females. In any case, it is safe to conclude that the developmental trajectory of AMPA/NMDA ratios highly depends on the brain region.

The sex-specific maturation extended to sEPSCs whose amplitude augmented in adult females in keeping with the accompanying maturation of dendritic spines in this group (see below).

SEPSCs' properties remain overall comparable across sexes during maturation, suggesting that AMPA currents play a minor role in the high AMPA/NMDA ratios measured in pubescent males. In the BA of adult rats, mEPSCs' frequency was increased when females were in diestrus but comparable to males while in proestrus (Blume et. al, 2017), leading to an overall increase in mEPSCs' frequency in females compared with males, while mEPSCs' amplitudes were similar. We did not observe such sex difference perhaps because of several methodological differences: our experiments were blind to the estrous cycle; we used coronal vs horizontal brain slices, we favored K^+Gluconate internal medium over Cesium based solution, and we recorded spontaneous activity in the presence or absence of TTX.

Interestingly, Blume and coworkers correlated this sex-specific increase in frequency with an increase in spine density in females (independently of estrous cycle), while in our hands the lack of sex-differences in sEPSCs was accompanied by stable dendritic spine density. Thus, the studies are divergent with one another, but coherent on their own, pointing to the possibility that somewhat different populations of neurons/dendrites were recorded/reconstructed. In

support of this idea, one must note that Blume and coworkers discarded non pyramidal shaped neurons while we exploited all glutamatergic principal neurons, from stellate to pyramidal (See methods).

Dendritic spines

Our results replicate and extend upon previous morphological reconstructions of BLA principal neurons in male rats and mice showing that spine density remained stable between pubescence and adulthood (Bosch & Ehrlich, 2015; Ryan et al., 2016), by demonstrating that this remains the case in females. Although we elected not to formally classify spines into the classical categories (thin, stubby, mushroom), the majority of spines identified in our rat groups were clearly thin as previously showed in the BLA (J.-Y. Zhang et al., 2019). Quantitative analysis of our data revealed a remodeling of dendritic spines after puberty, particularly in females. Principal neurons of pubescent females had shorter spine lengths, but larger spine head diameters and spine volumes. In the BLA, large spine head diameters do not correlate with large EPSC amplitude (J.-Y. Zhang et al., 2019), in agreement with the current lack of difference in sEPSCs amplitude in adults of both sexes (see above).

Sex influences the maturational profiles of LTP and LTD.

The synaptic repertoire NMDAR is an important determinant of synaptic plasticity (Paoletti et al., 2013). Notably, in the BLA of young male rats (PND-17-24), GluN2A- and GluN2B-containing NMDAR subunits underlie LTP and LTD at auditory thalamic-LA pathway, respectively (Dalton et al., 2012). NMDAR activity or subunits mRNA expression can be modulated by gonadectomy in males (van den Buuse et al., 2017), estrous cycle in females (Picard et al., 2019), or sex (Damborsky & Winzer-Serhan, 2012; Qi et al., 2016). In the BLA, a recent study (Guadagno et al., 2020) did not report sex-differences in NMDAR and AMPAR subunit protein levels in pre-pubertal rats, but showed a sex-dependent shift of protein levels in response to stress. While the developmental decrease of synaptic GluN2B-containing NMDARs is completed by the second post-natal week in certain areas such as the hippocampus and the NAc (Bellone & Nicoll, 2007; Chavis & Westbrook, 2001; Kasanetz & Manzoni, 2009; Mierau et al., 2004), it is delayed towards adulthood in the PFC (Iafrati et al., 2016), suggesting that NMDAR composition can fluctuate late in development. Altogether, these data suggest that the sex-dependent divergent maturational trajectories of LTP and LTD could be influenced by sex-specific maturation of NMDAR subtypes in the BLA.

TBS specifically failed to induce LTP in the BLA of adult females. Compelling evidence indicate sex-differences in LTP and learning (Gall et al., 2021). Several studies reported stronger LTP in males in the hippocampus of adult mice, while a five-paired theta burst akin to ours failed to induce LTP in female though triggered a robust LTP in males; conversely, a 10-paired TBS protocol induced LTP in both sexes, suggesting a higher threshold for LTP induction in females (W. Wang et al., 2018). Thus, in the CNS, sex-differences in LTP are commonly observed and the BLA is no exception.

Finally, LFS-LTD was present throughout maturation in females, but only emerged at adulthood in males. Interestingly, GABAergic inhibition is necessary to induce LFS-LTD in the BLA (Rammes et al., 2001). Even though GABAergic basic synaptic properties are mature at adolescence (Ehrlich et al., 2013), there is evidence showing that BLA circuits are less inhibited in adolescent pre-pubertal male rats (-PND40) than in adults (Selleck et al., 2018; W. Zhang & Rosenkranz, 2012). In addition, early stress exposure enhances LFS-LTD in the BLA (Danielewicz & Hess, 2014). In the hippocampus, stress exposure only enhances LTD in males in early adolescence and this is concomitant with sex-differences in both basal level of circulating corticosteroids and glucocorticoid receptors expression (Huang et al., 2012). Thus,

potential lines of research to elucidate the mechanisms preventing LTD in pubescent males include GABAergic system and glucocorticoids.

In conclusion, these data illustrate how male and female rats follow divergent maturational trajectories and identify previously unreported sex-differences at adulthood. Taken together with previous work (Blume et al., 2017, 2019; Hetzel & Rosenkranz, 2014), this study highlights the complexity of the cellular substrates to the BLA linked sex-specific behaviors at adolescence and adulthood.
Both a bigger range of behavioral studies as well as extended characterizations of plasticity and synaptic functions in animals of both sexes in other brain regions are necessary to better understand how sex-differences influence brain functions and behavior.

Author contributions:
Pauline Guily: Conceptualization; Data curation; Formal analysis; Validation; Writing: review and editing.
Olivier Lassalle: Data curation; Formal analysis; Validation; Methodology.
Olivier JJ Manzoni: Conceptualization; Supervision; Funding acquisition; Methodology; Writing: original draft, review and editing; Project administration.

Funding and Disclosures:
This work was supported by the Institut National de la Santé et de la Recherche Médicale (INSERM); Fondation pour la Recherche Médicale (Equipe FRM 2015 to O.M.) and the NIH (R01DA043982 to O.M.).

Declarations of interest: The authors declare no competing interests.

Acknowledgements: The authors are grateful to the Chavis-Manzoni team members for helpful discussions and to Dr. A.F. Scheyer for critical reading and help with writing the manuscript.

References

Bara, A., Manduca, A., Bernabeu, A., Borsoi, M., Serviado, M., Lassalle, O., Murphy, M., Wager-Miller, J., Mackie, K., Pelissier-Alicot, A.-L., Trezza, V., & Manzoni, O. J. (2018). Sex-dependent effects of in utero cannabinoid exposure on cortical function. *ELife*, *7*. https://doi.org/10.7554/eLife.36234

Bellone, C., & Nicoll, R. A. (2007). Rapid Bidirectional Switching of Synaptic NMDA Receptors. *Neuron*, *55*(5), 779-785. https://doi.org/10.1016/j.neuron.2007.07.035

Bender, R. A., Zhou, L., Vierk, R., Brandt, N., Keller, A., Gee, C. E., Schäfer, M. K. E., & Rune, G. M. (2017). Sex-Dependent Regulation of Aromatase-Mediated Synaptic Plasticity in the Basolateral Amygdala. *The Journal of Neuroscience*, *37*(6), 1532-1545. https://doi.org/10.1523/JNEUROSCI.1532-16.2016

Bernabeu, A., Bara, A., Manduca, A., Borsoi, M., Lassalle, O., Pelissier-Alicot, A.-L., & Manzoni, O. J. (2020). *Sex-specific maturational trajectory of endocannabinoid plasticity in the rat prefrontal cortex* [Preprint]. Neuroscience. https://doi.org/10.1101/2020.10.09.332965

Blume, S. R., Freedberg, M., Vantrease, J. E., Chan, R., Padival, M., Record, M. J., DeJoseph, M. R., Urban, J. H., & Rosenkranz, J. A. (2017). Sex- and Estrus-Dependent Differences in Rat Basolateral Amygdala. *The Journal of Neuroscience*, *37*(44), 10567-10586. https://doi.org/10.1523/JNEUROSCI.0758-17.2017

Blume, S. R., Padival, M., Urban, J. H., & Rosenkranz, J. A. (2019). Disruptive effects of repeated stress on basolateral amygdala neurons and fear behavior across the estrous cycle in rats. *Scientific Reports*, *9*(1), 12292. https://doi.org/10.1038/s41598-019-48683-3

Bocchio, M., Nabavi, S., & Capogna, M. (2017). Synaptic Plasticity, Engrams, and Network Oscillations in Amygdala Circuits for Storage and Retrieval of Emotional Memories. *Neuron*, *94*(4), 731-743. https://doi.org/10.1016/j.neuron.2017.03.022

Borsoi, M., Manduca, A., Bara, A., Lassalle, O., Pelissier-Alicot, A.-L., & Manzoni, O. J. (2019). Sex Differences in the Behavioral and Synaptic Consequences of a Single in vivo Exposure to the Synthetic Cannabimimetic WIN55,212-2 at Puberty and Adulthood. *Frontiers in Behavioral Neuroscience*, *13*, 23. https://doi.org/10.3389/fnbeh.2019.00023

Bosch, D., & Ehrlich, I. (2015). Postnatal maturation of GABAergic modulation of sensory inputs onto lateral amygdala principal neurons : Development of sensory input inhibition in mouse lateral amygdala. *The Journal of Physiology*, *593*(19), 4387-4409. https://doi.org/10.1113/JP270645

Bramen, J. E., Hranilovich, J. A., Dahl, R. E., Forbes, E. E., Chen, J., Toga, A. W., Dinov, I. D., Worthman, C. M., & Sowell, E. R. (2011). Puberty Influences Medial Temporal Lobe and Cortical Gray Matter Maturation Differently in Boys Than Girls Matched for Sexual Maturity. *Cerebral Cortex*, *21*(3), 636-646. https://doi.org/10.1093/cercor/bhq137

Breslau, J., Gilman, S. E., Stein, B. D., Ruder, T., Gmelin, T., & Miller, E. (2017). Sex differences in recent first-onset depression in an epidemiological sample of adolescents. *Translational Psychiatry*, *7*(5), e1139-e1139. https://doi.org/10.1038/tp.2017.105

Brinley-Reed, M., Mascagni, F., & McDonald, A. J. (1995). Synaptology of prefrontal cortical projections to the basolateral amygdala : An electron microscopic study in the rat. *Neuroscience Letters*, *202*(1), 45-48. https://doi.org/10.1016/0304-3940(95)12212-5

Cahill, L., Uncapher, M., Kilpatrick, L., Alkire, M. T., & Turner, J. (2004). Sex-Related Hemispheric Lateralization of Amygdala Function in Emotionally Influenced Memory : An fMRI Investigation. *Learning & Memory*, *11*(3), 261-266. https://doi.org/10.1101/lm.70504

Canli, T., Desmond, J. E., Zhao, Z., & Gabrieli, J. D. E. (2002). Sex differences in the neural basis of emotional memories. *Proceedings of the National Academy of Sciences*, *99*(16), 10789-10794. https://doi.org/10.1073/pnas.162356599
Casey, B. J., Jones, R. M., & Hare, T. A. (2008). The Adolescent Brain. *Annals of the New York Academy of Sciences*, *1124*, 111-126. https://doi.org/10.1196/annals.1440.010
Chavis, P., & Westbrook, G. (2001). Integrins mediate functional pre- and postsynaptic maturation at a hippocampal synapse. *Nature*, *411*(6835), 317-321. https://doi.org/10.1038/35077101
Chen, J. C. T., & Lang, E. J. (2003). Inhibitory control of rat lateral amygdaloid projection cells. *Neuroscience*, *121*(1), 155-166. https://doi.org/10.1016/S0306-4522(03)00430-5
Christiansen, D. M., & Berke, E. T. (2020). Gender- and Sex-Based Contributors to Sex Differences in PTSD. *Current Psychiatry Reports*, *22*(4), 19. https://doi.org/10.1007/s11920-020-1140-y
Dalpian, F., Rasia-Filho, A. A., & Calcagnotto, M. E. (2019). Sexual dimorphism, estrous cycle and laterality determine the intrinsic and synaptic properties of medial amygdala neurons in rat. *Journal of Cell Science*, *132*(9), jcs227793. https://doi.org/10.1242/jcs.227793
Dalton, G. L., Wu, D. C., Wang, Y. T., Floresco, S. B., & Phillips, A. G. (2012). NMDA GluN2A and GluN2B receptors play separate roles in the induction of LTP and LTD in the amygdala and in the acquisition and extinction of conditioned fear. *Neuropharmacology*, *62*(2), 797-806. https://doi.org/10.1016/j.neuropharm.2011.09.001
Damborsky, J. C., & Winzer-Serhan, U. H. (2012). Effects of sex and chronic neonatal nicotine treatment on NKCC1, KCC2, BDNF, NR2A and NR2B mRNA expression in the postnatal rat hippocampus. *Neuroscience*, *225*, 105-117. https://doi.org/10.1016/j.neuroscience.2012.09.002
Danielewicz, J., & Hess, G. (2014). Early life stress alters synaptic modification range in the rat lateral amygdala. *Behavioural Brain Research*, *265*, 32-37. https://doi.org/10.1016/j.bbr.2014.02.012
Daviu, N., Bruchas, M. R., Moghaddam, B., Sandi, C., & Beyeler, A. (2019). Neurobiological links between stress and anxiety. *Neurobiology of Stress*, *11*, 100191. https://doi.org/10.1016/j.ynstr.2019.100191
Debanne, D., & Poo, M.-M. (2010). Spike-timing dependent plasticity beyond synapse—Pre- and post-synaptic plasticity of intrinsic neuronal excitability. *Frontiers in Synaptic Neuroscience*, *2*, 21. https://doi.org/10.3389/fnsyn.2010.00021
Ehrlich, D. E., Ryan, S. J., Hazra, R., Guo, J.-D., & Rainnie, D. G. (2013). Postnatal maturation of GABAergic transmission in the rat basolateral amygdala. *Journal of Neurophysiology*, *110*(4), 926-941. https://doi.org/10.1152/jn.01105.2012
Ehrlich, D. E., Ryan, S. J., & Rainnie, D. G. (2012). Postnatal development of electrophysiological properties of principal neurons in the rat basolateral amygdala : Development of principal neuron electrophysiology in the rat basolateral amygdala. *The Journal of Physiology*, *590*(19), 4819-4838. https://doi.org/10.1113/jphysiol.2012.237453
Faber, E. S. L., Callister, R. J., & Sah, P. (2001). Morphological and Electrophysiological Properties of Principal Neurons in the Rat Lateral Amygdala In Vitro. *Journal of Neurophysiology*, *85*(2), 714-723. https://doi.org/10.1152/jn.2001.85.2.714
Faber, E. S. L., & Sah, P. (2002). Physiological Role of Calcium-Activated Potassium Currents in the Rat Lateral Amygdala. *Journal of Neuroscience*, *22*(5), 1618-1628. https://doi.org/10.1523/JNEUROSCI.22-05-01618.2002
Farb, C., Aoki, C., Milner, T., Kaneko, T., & LeDoux, J. (1992). Glutamate immunoreactive

terminals in the lateral amygdaloid nucleus : A possible substrate for emotional memory. *Brain Research*, *593*(2), 145-158. https://doi.org/10.1016/0006-8993(92)91303-V
Gall, C. M., Le, A. A., & Lynch, G. (2021). Sex differences in synaptic plasticity underlying learning. *Journal of Neuroscience Research*, *0*(0), 1-19. https://doi.org/10.1002/jnr.24844
Geary, C. G., Wilk, V. C., Barton, K. L., Jefferson, P. O., Binder, T., Bhutani, V., Baker, C. L., Fernando-Peiris, A. J., Mousley, A. L., Rozental, S. F. A., Thompson, H. M., Touchon, J. C., Esteban, D. J., & Bergstrom, H. C. (2021). Sex differences in gut microbiota modulation of aversive conditioning, open field activity, and basolateral amygdala dendritic spine density. *Journal of Neuroscience Research*, *99*(7), 1780-1801. https://doi.org/10.1002/jnr.24848
Goddings, A.-L., Mills, K. L., Clasen, L. S., Giedd, J. N., Viner, R. M., & Blakemore, S.-J. (2014). The influence of puberty on subcortical brain development. *NeuroImage*, *88*, 242-251. https://doi.org/10.1016/j.neuroimage.2013.09.073
Graber, J. A. (2013). Pubertal timing and the development of psychopathology in adolescence and beyond. *Hormones and Behavior*, *64*(2), 262-269. https://doi.org/10.1016/j.yhbeh.2013.04.003
Greiner, E. M., Müller, I., Norris, M. R., Ng, K. H., & Sangha, S. (2019). Sex differences in fear regulation and reward-seeking behaviors in a fear-safety-reward discrimination task. *Behavioural Brain Research*, *368*, 111903. https://doi.org/10.1016/j.bbr.2019.111903
Gruene, T. M., Flick, K., Stefano, A., Shea, S. D., & Shansky, R. M. (2015). Sexually divergent expression of active and passive conditioned fear responses in rats. *eLife*, *4*, e11352. https://doi.org/10.7554/eLife.11352
Guadagno, A., Verlezza, S., Long, H., Wong, T. P., & Walker, C.-D. (2020). It Is All in the Right Amygdala : Increased Synaptic Plasticity and Perineuronal Nets in Male, But Not Female, Juvenile Rat Pups after Exposure to Early-Life Stress. *The Journal of Neuroscience*, *40*(43), 8276-8291. https://doi.org/10.1523/JNEUROSCI.1029-20.2020
Guo, Y., Liu, S., Cui, G.-B., Ma, L., Feng, B., Xing, J., Yang, Q., Li, X., Wu, Y., Xiong, L., Zhang, W., & Zhao, M. (2012). Acute stress induces down-regulation of large-conductance Ca2+-activated potassium channels in the lateral amygdala. *The Journal of Physiology*, *590*(4), 875-886. https://doi.org/10.1113/jphysiol.2011.223784
Hetzel, A., & Rosenkranz, J. A. (2014). Distinct Effects of Repeated Restraint Stress on Basolateral Amygdala Neuronal Membrane Properties in Resilient Adolescent and Adult Rats. *Neuropsychopharmacology*, *39*(9), 2114-2130. https://doi.org/10.1038/npp.2014.60
Huang, C.-C., Chen, J.-P., Yeh, C.-M., & Hsu, K.-S. (2012). Sex difference in stress-induced enhancement of hippocampal CA1 long-term depression during puberty. *Hippocampus*, *22*(7), 1622-1634. https://doi.org/10.1002/hipo.21003
Hunsberger, M. S., & Mynlieff, M. (2020). BK potassium currents contribute differently to action potential waveform and firing rate as rat hippocampal neurons mature in the first postnatal week. *Journal of Neurophysiology*, *124*(3), 703-714. https://doi.org/10.1152/jn.00711.2019
Hwang, E.-K., & Lupica, C. R. (2020). Altered Corticolimbic Control of the Nucleus Accumbens by Long-term Δ9-Tetrahydrocannabinol Exposure. *Biological Psychiatry*, *87*(7), 619-631. https://doi.org/10.1016/j.biopsych.2019.07.024
Iafrati, J., Malvache, A., Gonzalez Campo, C., Orejarena, M. J., Lassalle, O., Bouamrane, L., & Chavis, P. (2016). Multivariate synaptic and behavioral profiling reveals new developmental endophenotypes in the prefrontal cortex. *Scientific Reports*, *6*, 35504. https://doi.org/10.1038/srep35504
Janak, P. H., & Tye, K. M. (2015). From circuits to behaviour in the amygdala. *Nature*,

517(7534), 284-292. https://doi.org/10.1038/nature14188
Kasanetz, F., & Manzoni, O. J. (2009). Maturation of Excitatory Synaptic Transmission of the Rat Nucleus Accumbens From Juvenile to Adult. *Journal of Neurophysiology*, *101*(5), 2516-2527. https://doi.org/10.1152/jn.91039.2008
Kirshner, H., Aguet, F., Sage, D., & Unser, M. (2013). 3-D PSF fitting for fluorescence microscopy : Implementation and localization application. *Journal of Microscopy*, *249*(1), 13-25. https://doi.org/10.1111/j.1365-2818.2012.03675.x
Krężel, W., Dupont, S., Krust, A., Chambon, P., & Chapman, P. F. (2001). Increased anxiety and synaptic plasticity in estrogen receptor β-deficient mice. *Proceedings of the National Academy of Sciences*, *98*(21), 12278-12282. https://doi.org/10.1073/pnas.221451898
Kuehner, C. (2017). Why is depression more common among women than among men? *The Lancet Psychiatry*, *4*(2), 146-158. https://doi.org/10.1016/S2215-0366(16)30263-2
Labouesse, M. A., Lassalle, O., Richetto, J., Iafrati, J., Weber-Stadlbauer, U., Notter, T., Gschwind, T., Pujadas, L., Soriano, E., Reichelt, A. C., Labouesse, C., Langhans, W., Chavis, P., & Meyer, U. (2017). Hypervulnerability of the adolescent prefrontal cortex to nutritional stress via reelin deficiency. *Molecular Psychiatry*, *22*(7), 961-971. https://doi.org/10.1038/mp.2016.193
Lebron-Milad, K., & Milad, M. R. (2012). Sex differences, gonadal hormones and the fear extinction network : Implications for anxiety disorders. *Biology of Mood & Anxiety Disorders*, *2*, 3. https://doi.org/10.1186/2045-5380-2-3
Mahan, A. L., & Ressler, K. J. (2012). Fear conditioning, synaptic plasticity and the amygdala : Implications for posttraumatic stress disorder. *Trends in Neurosciences*, *35*(1), 24-35. https://doi.org/10.1016/j.tins.2011.06.007
Malenka, R. C., & Bear, M. F. (2004). LTP and LTD : An Embarrassment of Riches. *Neuron*, *44*(1), 5-21. https://doi.org/10.1016/j.neuron.2004.09.012
Malinow, R., & Malenka, R. C. (2002). AMPA Receptor Trafficking and Synaptic Plasticity. *Annual Review of Neuroscience*, *25*(1), 103-126. https://doi.org/10.1146/annurev.neuro.25.112701.142758
Manduca, A., Bara, A., Larrieu, T., Lassalle, O., Joffre, C., Layé, S., & Manzoni, O. J. (2017). Amplification of mGlu5-endocannabinoid signaling rescues behavioral and synaptic deficits in a mouse model of adolescent and adult dietary polyunsaturated fatty acid imbalance. *Journal of Neuroscience*, *37*(29), 6851-6868. https://doi.org/10.1523/JNEUROSCI.3516-16.2017
Martin, H. G. S., Lassalle, O., Brown, J. T., & Manzoni, O. J. (2016). Age-Dependent Long-Term Potentiation Deficits in the Prefrontal Cortex of the Fmr1 Knockout Mouse Model of Fragile X Syndrome. *Cerebral Cortex*, *26*(5), 2084-2092. https://doi.org/10.1093/cercor/bhv031
Matos, H. Y., Hernandez-Pineda, D., Charpentier, C. M., Rusk, A., Corbin, J. G., & Jones, K. S. (2020). Sex Differences in Biophysical Signatures across Molecularly Defined Medial Amygdala Neuronal Subpopulations. *ENeuro*, *7*(4). https://doi.org/10.1523/ENEURO.0035-20.2020
McLean, C. P., Asnaani, A., Litz, B. T., & Hofmann, S. G. (2011). Gender differences in anxiety disorders : Prevalence, course of illness, comorbidity and burden of illness. *Journal of Psychiatric Research*, *45*(8), 1027-1035. https://doi.org/10.1016/j.jpsychires.2011.03.006
Mierau, S. B., Meredith, R. M., Upton, A. L., & Paulsen, O. (2004). Dissociation of experience-dependent and -independent changes in excitatory synaptic transmission during development of barrel cortex. *Proceedings of the National Academy of Sciences*, *101*(43), 15518-15523. https://doi.org/10.1073/pnas.0402916101

Moyer, C. E., & Zuo, Y. (2018). Cortical dendritic spine development and plasticity : Insights from in vivo imaging. *Current Opinion in Neurobiology*, *53*, 76-82. https://doi.org/10.1016/j.conb.2018.06.002
Mozhui, K., Karlsson, R.-M., Kash, T. L., Ihne, J., Norcross, M., Patel, S., Farrell, M. R., Hill, E. E., Graybeal, C., Martin, K. P., Camp, M., Fitzgerald, P. J., Ciobanu, D. C., Sprengel, R., Mishina, M., Wellman, C. L., Winder, D. G., Williams, R. W., & Holmes, A. (2010). Strain Differences in Stress Responsivity Are Associated with Divergent Amygdala Gene Expression and Glutamate-Mediated Neuronal Excitability. *Journal of Neuroscience*, *30*(15), 5357-5367. https://doi.org/10.1523/JNEUROSCI.5017-09.2010
Nestler, E. J., Barrot, M., DiLeone, R. J., Eisch, A. J., Gold, S. J., & Monteggia, L. M. (2002). Neurobiology of Depression. *Neuron*, *34*(1), 13-25. https://doi.org/10.1016/S0896-6273(02)00653-0
Paoletti, P., Bellone, C., & Zhou, Q. (2013). NMDA receptor subunit diversity : Impact on receptor properties, synaptic plasticity and disease. *Nature Reviews Neuroscience*, *14*(6), 383-400. https://doi.org/10.1038/nrn3504
Pape, H.-C., & Pare, D. (2010). Plastic Synaptic Networks of the Amygdala for the Acquisition, Expression, and Extinction of Conditioned Fear. *Physiological Reviews*, *90*(2), 419-463. https://doi.org/10.1152/physrev.00037.2009
Patton, G. C., Olsson, C., Bond, L., Toumbourou, J. W., Carlin, J. B., Hemphill, S. A., & Catalano, R. F. (2008). PREDICTING FEMALE DEPRESSION ACROSS PUBERTY : A TWO-NATION LONGITUDINAL STUDY. *Journal of the American Academy of Child and Adolescent Psychiatry*, *47*(12), 1424-1432. https://doi.org/10.1097/CHI.0b013e3181886ebe
Phelps, E. A. (2004). Human emotion and memory : Interactions of the amygdala and hippocampal complex. *Current Opinion in Neurobiology*, *14*(2), 198-202. https://doi.org/10.1016/j.conb.2004.03.015
Picard, N., Takesian, A. E., Fagiolini, M., & Hensch, T. K. (2019). NMDA 2A receptors in parvalbumin cells mediate sex-specific rapid ketamine response on cortical activity. *Molecular Psychiatry*, *24*(6), 828-838. https://doi.org/10.1038/s41380-018-0341-9
Power, J. M., & Sah, P. (2008). Competition between Calcium-Activated K+ Channels Determines Cholinergic Action on Firing Properties of Basolateral Amygdala Projection Neurons. *Journal of Neuroscience*, *28*(12), 3209-3220. https://doi.org/10.1523/JNEUROSCI.4310-07.2008
Proaño, S. B., & Meitzen, J. (2020). Estradiol decreases medium spiny neuron excitability in female rat nucleus accumbens core. *Journal of Neurophysiology*, *123*(6), 2465-2475. https://doi.org/10.1152/jn.00210.2020
Proaño, S. B., Morris, H. J., Kunz, L. M., Dorris, D. M., & Meitzen, J. (2018). Estrous cycle-induced sex differences in medium spiny neuron excitatory synaptic transmission and intrinsic excitability in adult rat nucleus accumbens core. *Journal of Neurophysiology*, *120*(3), 1356-1373. https://doi.org/10.1152/jn.00263.2018
Przybysz, K. R., Gamble, M. E., & Diaz, M. R. (2021). Moderate adolescent chronic intermittent ethanol exposure sex-dependently disrupts synaptic transmission and kappa opioid receptor function in the basolateral amygdala of adult rats. *Neuropharmacology*, *188*, 108512. https://doi.org/10.1016/j.neuropharm.2021.108512
Qi, X., Zhang, K., Xu, T., Yamaki, V. N., Wei, Z., Huang, M., Rose, G. M., & Cai, X. (2016). Sex Differences in Long-Term Potentiation at Temporoammonic-CA1 Synapses : Potential Implications for Memory Consolidation. *PLOS ONE*, *11*(11), e0165891. https://doi.org/10.1371/journal.pone.0165891

Radley, J. J., Farb, C. R., He, Y., Janssen, W. G. M., Rodrigues, S. M., Johnson, L. R., Hof, P. R., LeDoux, J. E., & Morrison, J. H. (2007). Distribution of NMDA and AMPA receptor subunits at thalamo-amygdaloid dendritic spines. *Brain Research*, *1134*, 87-94. https://doi.org/10.1016/j.brainres.2006.11.045

Rammes, G., Eder, M., Dodt, H.-U., Kochs, E., & Zieglgänsberger, W. (2001). Long-term depression in the basolateral amygdala of the mouse involves the activation of interneurons. *Neuroscience*, *107*(1), 85-97. https://doi.org/10.1016/S0306-4522(01)00336-0

Rau, A. R., Chappell, A. M., Butler, T. R., Ariwodola, O. J., & Weiner, J. L. (2015). Increased Basolateral Amygdala Pyramidal Cell Excitability May Contribute to the Anxiogenic Phenotype Induced by Chronic Early-Life Stress. *Journal of Neuroscience*, *35*(26), 9730-9740. https://doi.org/10.1523/JNEUROSCI.0384-15.2015

Rosenkranz, J. A., Venheim, E. R., & Padival, M. (2010). Chronic Stress Causes Amygdala Hyperexcitability in Rodents. *Biological Psychiatry*, *67*(12), 1128-1136. https://doi.org/10.1016/j.biopsych.2010.02.008

Ryan, S. J., Ehrlich, D. E., & Rainnie, D. G. (2016). Morphology and dendritic maturation of developing principal neurons in the rat basolateral amygdala. *Brain Structure and Function*, *221*(2), 839-854. https://doi.org/10.1007/s00429-014-0939-x

Sage, D., Donati, L., Soulez, F., Fortun, D., Schmit, G., Seitz, A., Guiet, R., Vonesch, C., & Unser, M. (2017). DeconvolutionLab2 : An open-source software for deconvolution microscopy. *Methods*, *115*, 28-41. https://doi.org/10.1016/j.ymeth.2016.12.015

Sah, P., & Louise Faber, E. S. (2002). Channels underlying neuronal calcium-activated potassium currents. *Progress in Neurobiology*, *66*(5), 345-353. https://doi.org/10.1016/S0301-0082(02)00004-7

Scherf, K. S., Smyth, J. M., & Delgado, M. R. (2013). The amygdala : An agent of change in adolescent neural networks. *Hormones and Behavior*, *64*(2), 298-313. https://doi.org/10.1016/j.yhbeh.2013.05.011

Scheyer, A. F., Borsoi, M., Pelissier-Alicot, A.-L., & Manzoni, O. J. J. (2020a). Maternal Exposure to the Cannabinoid Agonist WIN 55,12,2 during Lactation Induces Lasting Behavioral and Synaptic Alterations in the Rat Adult Offspring of Both Sexes. *ENeuro*, *7*(5). https://doi.org/10.1523/ENEURO.0144-20.2020

Scheyer, A. F., Borsoi, M., Pelissier-Alicot, A.-L., & Manzoni, O. J. J. (2020b). Perinatal THC exposure via lactation induces lasting alterations to social behavior and prefrontal cortex function in rats at adulthood. *Neuropsychopharmacology: Official Publication of the American College of Neuropsychopharmacology*, *45*(11), 1826-1833. https://doi.org/10.1038/s41386-020-0716-x

Scheyer, A. F., Borsoi, M., Wager-Miller, J., Pelissier-Alicot, A.-L., Murphy, M. N., Mackie, K., & Manzoni, O. J. J. (2019). Cannabinoid exposure via lactation in rats disrupts perinatal programming of the GABA trajectory and select early-life behaviors. *Biological Psychiatry*, Epub ahead of print. https://doi.org/10.1016/j.biopsych.2019.08.023

Schneider, M. (2013). Adolescence as a vulnerable period to alter rodent behavior. *Cell and Tissue Research*, *354*(1), 99-106. https://doi.org/10.1007/s00441-013-1581-2

Selleck, R. A., Zhang, W., Samberg, H. D., Padival, M., & Rosenkranz, J. A. (2018). Limited prefrontal cortical regulation over the basolateral amygdala in adolescent rats. *Scientific Reports*, *8*(1), 17171. https://doi.org/10.1038/s41598-018-35649-0

Shansky, R. M., & Murphy, A. Z. (2021). Considering sex as a biological variable will require a global shift in science culture. *Nature Neuroscience*, *24*(4), 457-464. https://doi.org/10.1038/s41593-021-00806-8

Spear, L. P. (2000). The adolescent brain and age-related behavioral manifestations. *Neuroscience & Biobehavioral Reviews*, *24*(4), 417-463. https://doi.org/10.1016/S0149-7634(00)00014-2
Thomazeau, A., Lassalle, O., Iafrati, J., Souchet, B., Guedj, F., Janel, N., Chavis, P., Delabar, J., & Manzoni, O. J. (2014). Prefrontal deficits in a murine model overexpressing the down syndrome candidate gene dyrk1a. *The Journal of Neuroscience: The Official Journal of the Society for Neuroscience*, *34*(4), 1138-1147. https://doi.org/10.1523/JNEUROSCI.2852-13.2014
van den Buuse, M., Low, J. K., Kwek, P., Martin, S., & Gogos, A. (2017). Selective enhancement of NMDA receptor-mediated locomotor hyperactivity by male sex hormones in mice. *Psychopharmacology*, *234*(18), 2727-2735. https://doi.org/10.1007/s00213-017-4668-8
Wang, S.-J., & Gean, P.-W. (1999). Long-Term Depression of Excitatory Synaptic Transmission in the Rat Amygdala. *Journal of Neuroscience*, *19*(24), 10656-10663. https://doi.org/10.1523/JNEUROSCI.19-24-10656.1999
Wang, W., Le, A. A., Hou, B., Lauterborn, J. C., Cox, C. D., Levin, E. R., Lynch, G., & Gall, C. M. (2018). Memory-Related Synaptic Plasticity Is Sexually Dimorphic in Rodent Hippocampus. *Journal of Neuroscience*, *38*(37), 7935-7951. https://doi.org/10.1523/JNEUROSCI.0801-18.2018
Washburn, M., & Moises, H. (1992). Electrophysiological and morphological properties of rat basolateral amygdaloid neurons in vitro. *The Journal of Neuroscience*, *12*(10), 4066-4079. https://doi.org/10.1523/JNEUROSCI.12-10-04066.1992
Yang, R., Zhang, B., Chen, T., Zhang, S., & Chen, L. (2017). Postpartum estrogen withdrawal impairs GABAergic inhibition and LTD induction in basolateral amygdala complex via down-regulation of GPR30. *European Neuropsychopharmacology*, *27*(8), 759-772. https://doi.org/10.1016/j.euroneuro.2017.05.010
Zhang, J.-Y., Liu, T.-H., He, Y., Pan, H.-Q., Zhang, W.-H., Yin, X.-P., Tian, X.-L., Li, B.-M., Wang, X.-D., Holmes, A., Yuan, T.-F., & Pan, B.-X. (2019). Chronic Stress Remodels Synapses in an Amygdala Circuit–Specific Manner. *Biological Psychiatry*, *85*(3), 189-201. https://doi.org/10.1016/j.biopsych.2018.06.019
Zhang, W., & Rosenkranz, J. A. (2012). Repeated restraint stress increases basolateral amygdala neuronal activity in an age-dependent manner. *Neuroscience*, *226*, 459-474. https://doi.org/10.1016/j.neuroscience.2012.08.051
Zhang, Y., Garcia, E., Sack, A.-S., & Snutch, T. P. (2020). L-type calcium channel contributions to intrinsic excitability and synaptic activity during basolateral amygdala postnatal development. *Journal of Neurophysiology*, *123*(3), 1216-1235. https://doi.org/10.1152/jn.00606.2019

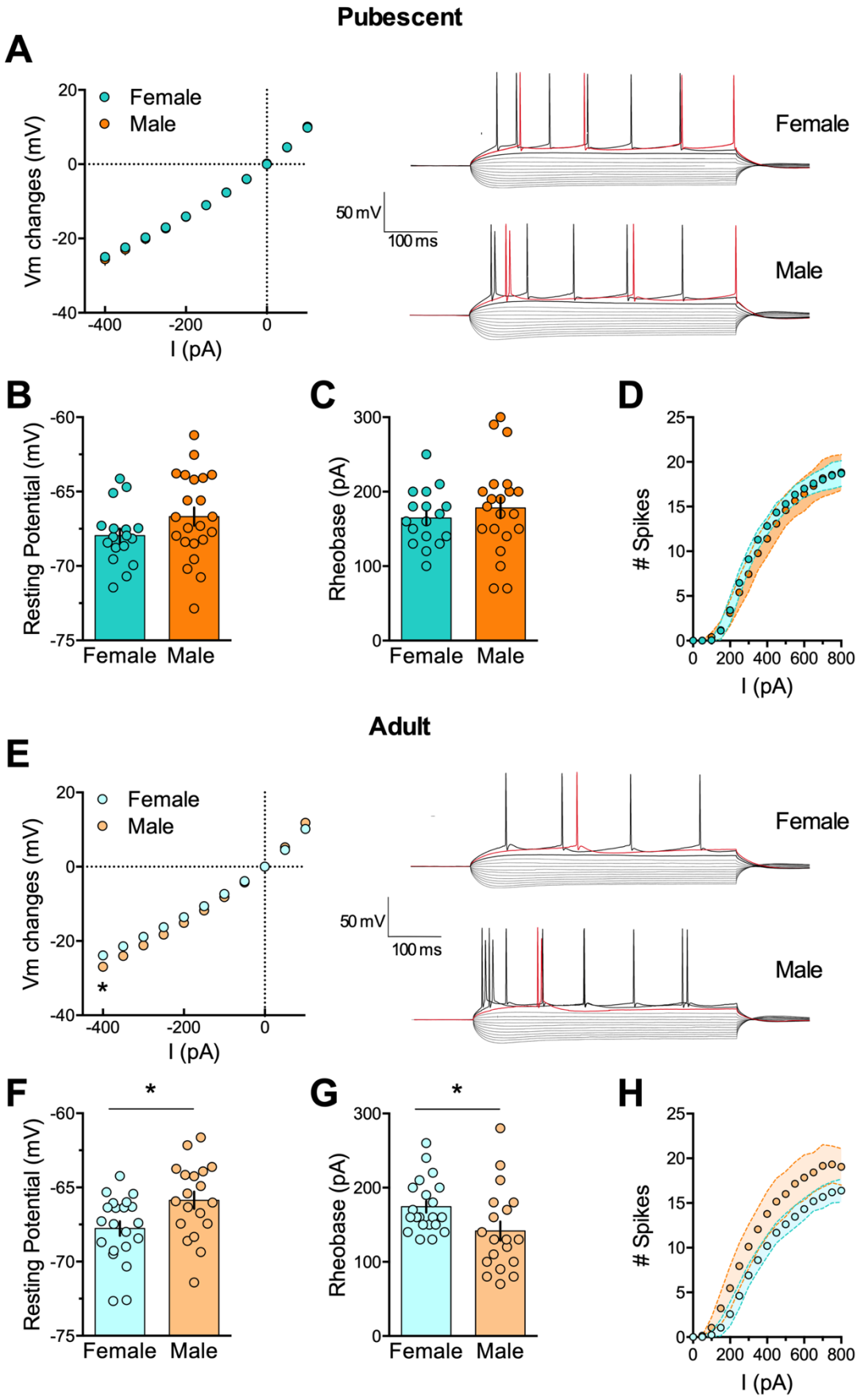
Pubescent
A
Female
Male
Vm changes (mV)
I (pA)
50 mV
100 ms
Female
Male
B
Resting Potential (mV)
Female
Male
C
Rheobase (pA)
Female
Male
D
Spikes
I (pA)
Adult
E
Female
Male
Vm changes (mV)
I (pA)
50 mV
100 ms
Female
Male
F
Resting Potential (mV)
Female
Male
G
Rheobase (pA)
Female
Male
H
Spikes
I (pA)

Figure 1: Sex-specific differences in intrinsic properties of rat BLA principal neurons emerge in adulthood.

A-D: BLA neurons in female and male pubescent rats have similar intrinsic properties. (A) Left, current–voltage (I-V) curves from BLA pyramidal neurons were similar in pubescent females (blue) and pubescent males (orange) (Two-way repeated measures ANOVA: $F_{(interaction\ 10, 370)} = 0.05698$ $P > 0.9999$). Right, typical membrane response to current steps of 50 pA from -400 pA to 250 pA in neurons of pubescent females (top) and males (bottom). (B) No difference was observed in the resting membrane potential of male and female pubescent rats (Mann–Whitney U test: W = 128.5 P = 0.099). (C) Progressive current injections in 10pA steps revealed that the minimal current required to trigger an action potential (i.e., rheobase) did not differ between male and female pubescent rats (Mann–Whitney U test: W = 150 P = 0.410). (D) The number of evoked action potentials in response to increasing depolarizing current step was similar in pubescent rats of both sexes (Two-way repeated measures ANOVA: $F_{(interaction\ 16,592)} = 0.957$, $P = 0.504$). Pubescent: female, n = 17 cells/10rats; male, n = 22 cells/11 rats. ***E-H: Sex specific intrinsic properties of BLA neurons in adult rats.*** (E) Left, IV curves of BLA pyramidal neurons were similar in adult females (blue) and adult males (orange) (Two-way repeated measures ANOVA: $F_{(interaction\ 10, 380)} = 2.906$ $P = 0.0016$, $F_{(sex\ 1, 38)} = 3.033$ $P = 0.0897$). Right, typical membrane response to current steps of 50 pA from -400 pA to 250 pA in neurons of females (top) and males (bottom). (F) The membrane potential of BLA neurons in adult males was hyperpolarized compared to adult females (Mann–Whitney U test: W = 111 P = 0.016). (G) The rheobase of BLA pyramidal neurons was lower in adult males than in adult females (Mann–Whitney U test: W = 106 P = 0.017). (H) The number of evoked action potentials was also higher in adult males compared to adult females (Two-way repeated measures ANOVA: $F_{(interaction\ 16,608)} = 3.535$, $P < 0.001$, $F_{(sex\ 1,38)} = 8.291$, $P = 0.007$). Adult: female, n = 21 cells/12rats; male, n = 22 cells/11 rats. Individual point in scatter dot plots represents one cell. All data are shown as mean ± SEM, except (D) and (H) mean ± 95% of CI. *P<0.05.

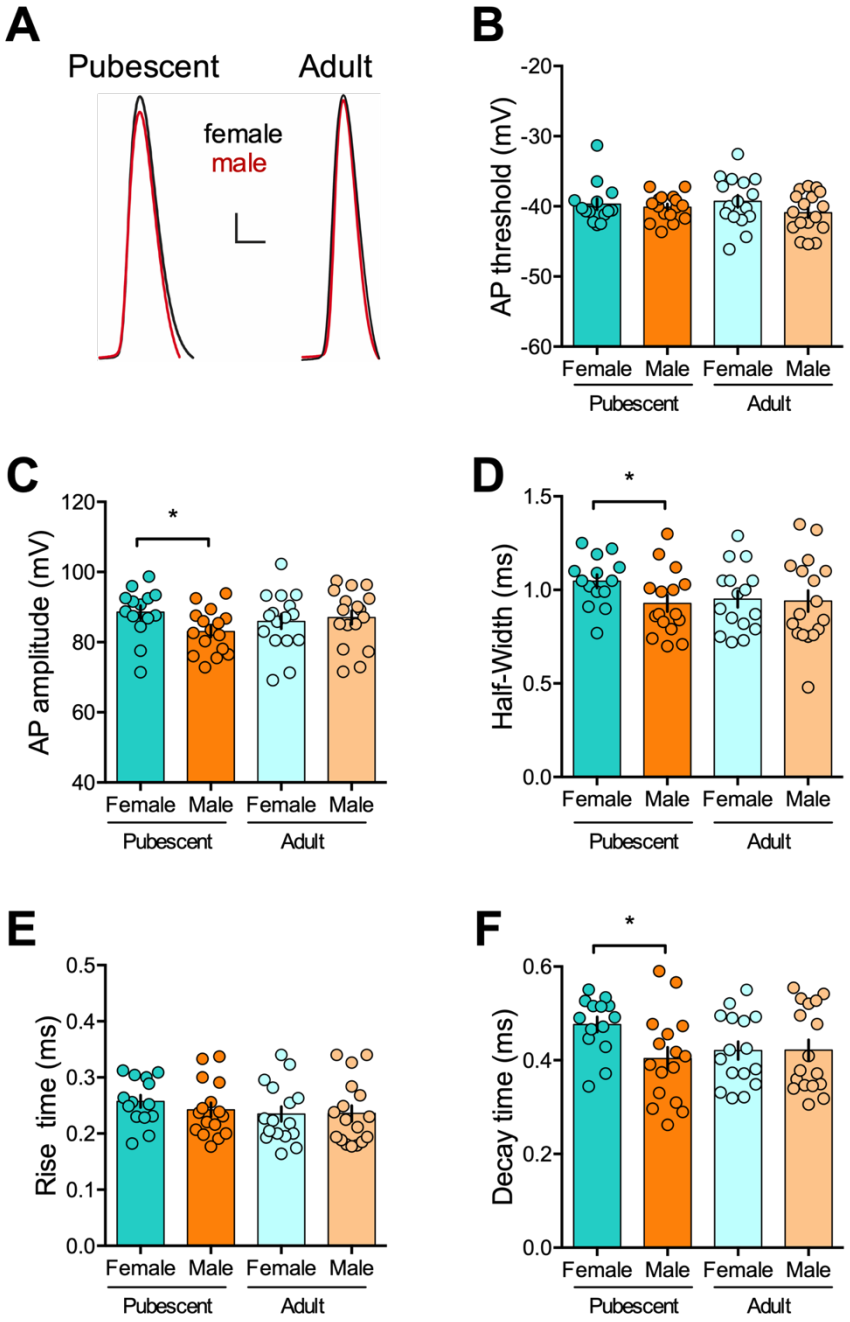
A
Pubescent
Adult
female
male
B
AP threshold (mV)
-20
-30
-40
-50
-60
Female
Male
Female
Male
Pubescent
Adult
C
AP amplitude (mV)
120
100
80
60
40
*
Female
Male
Female
Male
Pubescent
Adult
D
Half-Width (ms)
1.5
1.0
0.5
0.0
*
Female
Male
Female
Male
Pubescent
Adult
E
Rise time (ms)
0.5
0.4
0.3
0.2
0.1
0.0
Female
Male
Female
Male
Pubescent
Adult
F
Decay time (ms)
0.6
0.4
0.2
0.0
*
Female
Male
Female
Male
Pubescent
Adult

Figure 2: Action potential properties of principal neurons in the rat BLA

(**A**) Representative traces of the first spike elicited by a 10 pA current step injection in neurons of pubescent (right) and adult (left) rats. Male (red) and female (black) traces are superimposed for each age group. Scale bar :10 mV, 1ms. (**B**) Action potential threshold did not vary between groups. (**C**) In pubescent rats, action potentials were of lower amplitude in males compared with females (Mann–Whitney U test: W = 56.50 P = 0.02). This sex-difference was not found in adults (Mann–Whitney U test: W = 121 P = 0.6). (**D**) Similarly, half-width was shorter in pubescent males compared with females (Mann–Whitney U test: W = 62 P = 0.037). No difference was found in the half-width of action potentials from neurons obtained either from male or female adult rats (Mann–Whitney U test: W = 134.5 P = 0.965). (**E**) Rise time was similar between each group. (**F**) Conversely, in the same way as for half-width, decay time was shorter in pubescent males compared with females whereas no difference was found between adult of both sexes (Mann–Whitney U test: pubescent, W = 57 P = 0.029; adult, W = 135 P = 0.986). Individual point in scatter dot plots represents one cell. All data are shown as mean ± SEM. *P<0.05. Pubescent: female, n = 14 cells/9 rats; male, n = 16cells/10 rats. Adult: female, n = 16cells/7 rats; male = 17cells/10 rats.

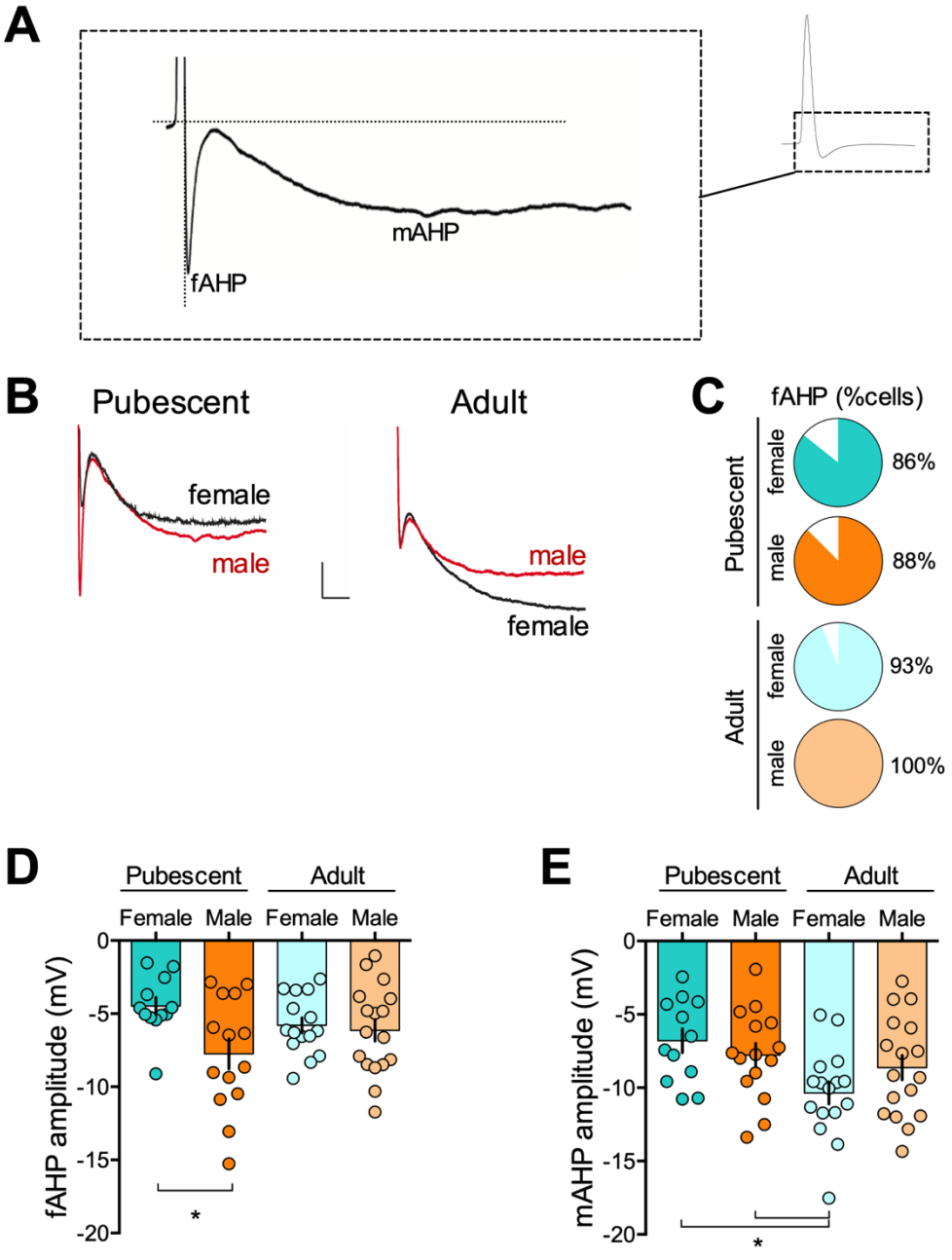
A
mAHP
fAHP
B
Pubescent
Adult
female
male
male
female
C
fAHP (%cells)
Pubescent
female
86%
male
88%
Adult
female
93%
male
100%
D
Pubescent
Adult
Female
Male
Female
Male
fAHP amplitude (mV)
0
-5
-10
-15
-20
*
E
Pubescent
Adult
Female
Male
Female
Male
mAHP amplitude (mV)
0
-5
-10
-15
-20
*

Figure 3: AHP profile of principal neurons in the rat BLA of pubescent and adult rat of both sexes

(**A**) Left, zoomed representation of the AHP of the action potential on the right. The fAHP is the local minimum directly following spike's repolarization within a couple of ms. The mAHP is a local minimum distinct from the fAHP and occurring 15-150 ms after the spike. (**B**) Representative traces of the first spike's AHP elicited by a 10 pA current step injection in neurons of pubescent (right) and adult (left) rats. Male (red) and female (black) traces are superimposed for each age group. Scale bar: 2 mV, 20ms. (**C**) Proportion of cells with a first spike expressing a fAHP in pubescent (female, dark blue, n = 12/14 cells, 86%; male, dark orange, n = 14/16, 88%,) and adult (female, light blue, n = 15/16, 93%; male, light orange, n = 17/17, 100%) rats. (**D**) The fAHP amplitude was significantly larger in pubescent males compared with females, whereas in adult rats the fAHP was of similar amplitude in males and females (Mann–Whitney U test: pubescent, W = 41 P = 0.026; adult, W = 114 P = 0.628). Pubescent: female, n = 12 cells/9 rats; male, n = 14 cells/10 rats. Adult: female, n = 15 cells/8 rats; male, n = 17 cells/10 rats. (**E**) The mAHP amplitude was significantly larger in adult females compared with pubescent males and females (Mann–Whitney U test: females, W = 34.5 P = 0.003; males, W = 111.5 P = 0.557). Pubescent: female, n = 12 cells/8 rats; male, n = 15 cells/9 rats. Adult: female, n = 16 cells/8 rats; male, n = 17 cells/10 rats. Individual point in scatter dot plots represents one cell. All data are shown as mean ± SEM. *P<0.05.

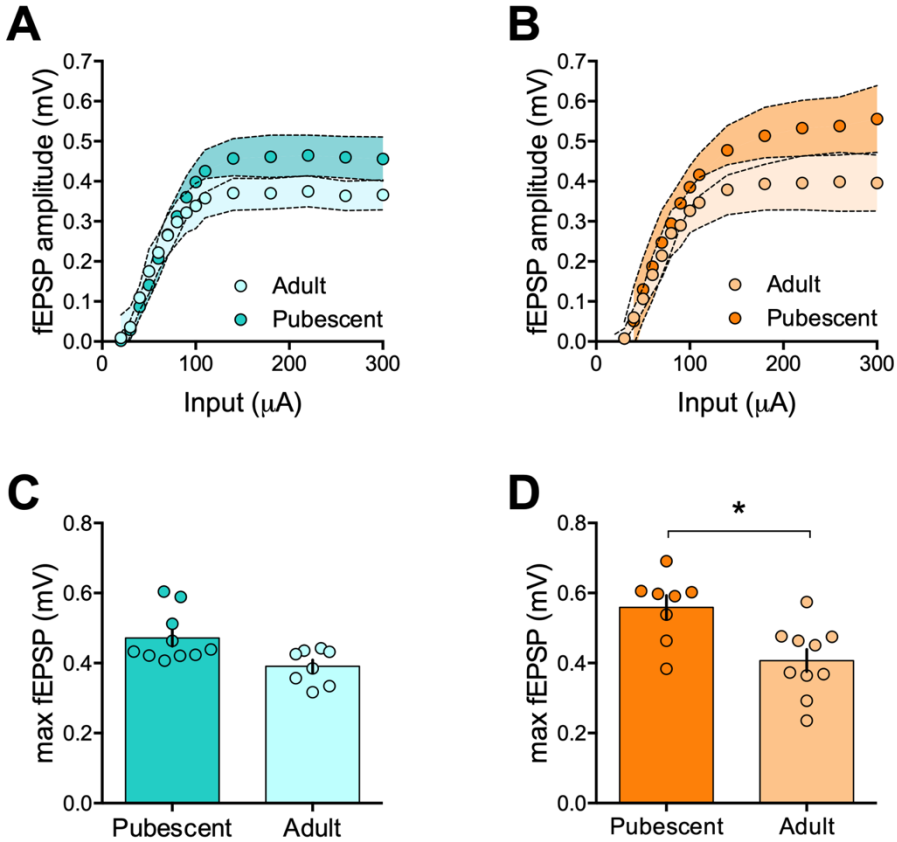
A
fEPSP amplitude (mV)
0.7
0.6
0.5
0.4
0.3
0.2
0.1
0.0
0
100
200
300
Input (μA)
Adult
Pubescent
B
fEPSP amplitude (mV)
Input (μA)
Adult
Pubescent
C
max fEPSP (mV)
0.8
0.6
0.4
0.2
0.0
Pubescent
Adult
D
*
max fEPSP (mV)
Pubescent
Adult

Figure 4: fEPSPs input-output profile

(**A-B**) Averaged fEPSP amplitude as a function of the stimulus intensity. There is a maturation of the input-output profile between pubescence and adulthood in both females (**A**; pubescent, n = 10; adult n = 8; Two-way repeated measures ANOVA: $F_{(interaction\ 14,224)} = 6.036$ $P < 0.0001$, $F_{(age\ 1,16)} = 2.694$ $P = 0.1203$) and males (**B**; pubescent, n = 8; adult n = 10; Two-way repeated measures ANOVA: $F_{(interaction\ 14,224)} = 5.289$ $P < 0.0001$, $F_{(age\ 14,224)} = 7.352$ $P = 0.0489$). (**C**) Maximum amplitude of fEPSPs elicited during the input-output did not differ between pubescent and adult females (Mann–Whitney U test: W = 19 P = 0.068) (**D**) Conversely, maximum amplitude of fEPSPs was significantly larger in slices obtained from pubescent males than in those obtained from adult males (Mann–Whitney U test: W = 9.5 P = 0.005). n = individual rats, one slice per rat. Data are shown as mean ±CI (A-B) or ± SEM (C-D). *P<0.05.

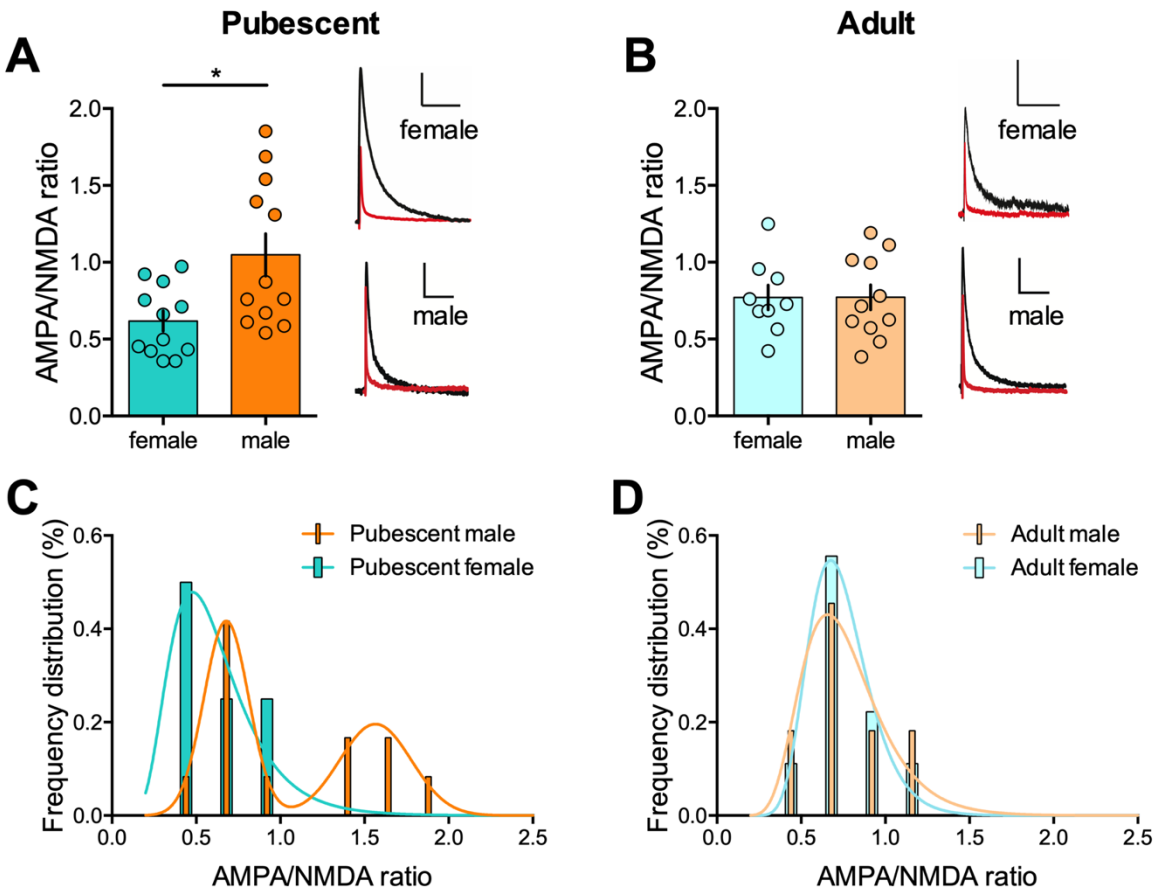
A
Pubescent
*
AMPA/NMDA ratio
2.0
1.5
1.0
0.5
0.0
female
male
female
male
B
Adult
AMPA/NMDA ratio
2.0
1.5
1.0
0.5
0.0
female
male
female
male
C
Frequency distribution (%)
0.6
0.4
0.2
0.0
Pubescent male
Pubescent female
0.0
0.5
1.0
1.5
2.0
2.5
AMPA/NMDA ratio
D
Frequency distribution (%)
0.6
0.4
0.2
0.0
Adult male
Adult female
0.0
0.5
1.0
1.5
2.0
2.5
AMPA/NMDA ratio

Figure 5: Sex-differences in AMPA/NMDA ratios disappear in adulthood

(A-B) Right: representative waveforms of AMPA EPSC evoked at +30mV in the presence of 50 μM APV (red) and NMDA EPSC obtained by digital subtraction of the AMPA component from the dual component EPSC evoked at +30mV (black). Scale bar: 500ms, 50 pA. (**A**) The AMPA/NMDA ratio of principal neurons was significantly higher in BLA slices obtained from pubescent males, as compared with those obtained from adult pubescent females (female, n = 12/6; male, n = 12/9; Mann–Whitney U test: W = 32 P = 0.02). (**B**) The AMPA/NMDA ratio did not differ in principal neurons of BLA slices obtained from adult males, as compared with those obtained from adult females (female, n = 9/6; male, n = 11/7; Mann–Whitney U test: W = 49 P > 0.999). **(C)** Frequency distribution of AMPA/NMDA ratio reveals a subset of neurons from pubescent males with AMPA/NMDA ratio comparable to pubescent females, and another population of neurons with a greater AMPA/NMDA ratio. AMPA/NMDA ratio data from pubescent females were best fit by a single Gaussian (blue line), whereas data from pubescent males were best fit by the sum of two Gaussians (orange line), indicative of two populations. **(D)** AMPA/NMDA ratio are distributed similarly between female and male adult rats. AMPA/NMDA ratio data of both groups best fit single gaussians. All data are shown as mean ± SEM. *P<0.05.

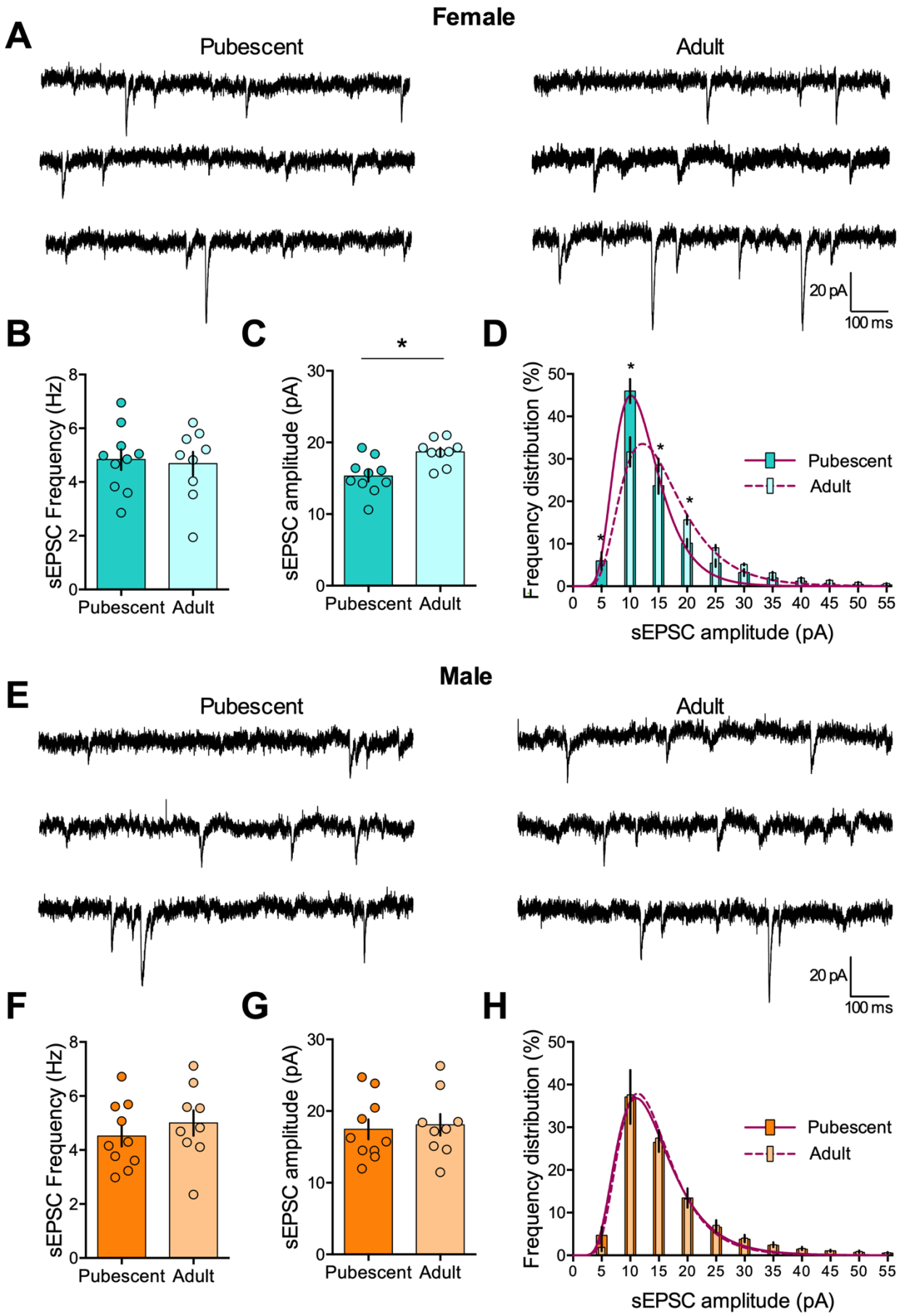
Female
A
Pubescent
Adult
20 pA
100 ms
B
sEPSC Frequency (Hz)
Pubescent
Adult
C
sEPSC amplitude (pA)
*
Pubescent
Adult
D
Frequency distribution (%)
Pubescent
Adult
sEPSC amplitude (pA)
Male
E
Pubescent
Adult
20 pA
100 ms
F
sEPSC Frequency (Hz)
Pubescent
Adult
G
sEPSC amplitude (pA)
Pubescent
Adult
H
Frequency distribution (%)
Pubescent
Adult
sEPSC amplitude (pA)

Figure 6: Amplitude distribution of sEPSCs is skewed towards larger amplitudes in adult females but not males BLA pyramidal neurons.

(A-D) sEPSCs are smaller in BLA pyramidal neurons of pubescent females compared with adult females. (A) Representative traces of sEPSCs recorded at -70 mV in BLA pyramidal neurons of female rats. (B) sEPSCs' mean frequency was similar in pubescent (n = 10 cells/8 rats, dark blue) and adult (n = 9 cells/7 rats, light blue) females (Mann–Whitney U test: W = 45 P > 0.999). (C) Adult females had a significantly greater amplitude of sEPSCs compared with pubescent females (Mann–Whitney U test: W = 12, P = 0.006). (D) Frequency distribution of individual sEPSCs' amplitude histogram reveals a higher proportion of large size events in adult compared to pubescent female rats (Two-way repeated measures ANOVA: $F_{(interaction\ 14,\ 255)}$ = 9.362, P < 0.0001). Log-normal curve fit showing distributions' distinct skewness between pubescent (solid line) and adult (dotted line) females. **(E-G) Amplitude and frequency of sEPSCs are similar in pubescent and adult males BLA pyramidal neurons.** (E) Representative traces of sEPSCs recorded at -70 mV in BLA pyramidal neurons of male rats. (F) sEPSCs' mean frequency was similar in pubescent (n = 10 cells/7 rats, dark orange) and adult (9 cells/7 rats, light orange) males (Mann–Whitney U test: W = 36, P = 0.497). (G) No difference was found in sEPSCs' average amplitude in pubescent and adult males (Mann–Whitney U test: W = 40, P = 0.720). (H) Individual sEPSCs' amplitudes are distributed similarly in pubescent and adult males (Two-way repeated measures ANOVA: $F_{(interaction\ 14,\ 255)}$ = 0.101, P > 0.9999). Log-normal curve fit showing distributions' similar skewness between pubescent (solid line) and adult (dotted line) males. All data are shown as mean ± SEM. *P<0.05.

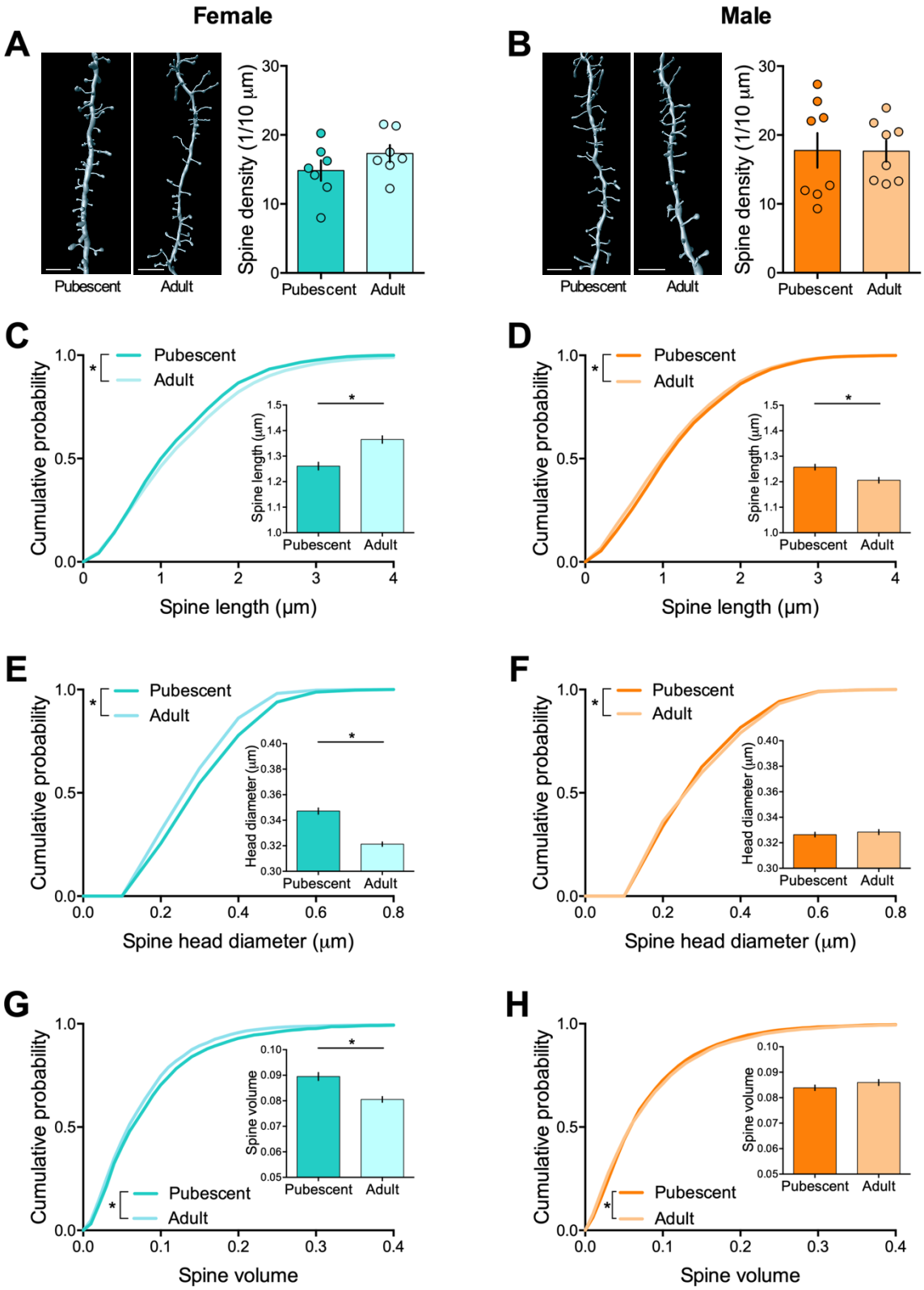
Female
Male
A
B
Pubescent
Adult
Spine density (1/10 µm)
C
D
E
F
G
H
Cumulative probability
Spine length (µm)
Spine head diameter (µm)
Spine volume
Head diameter (µm)
*

Figure 7: Sex-specific dendritic spine maturation of BLA principal neurons

(A) Left, representative 3D rendering of dendritic spines from neurobiotin filled principal neurons of female pubescent and adult rats. Scale bar: 4μm. Right, dendritic spine density was similar in pubescent (n = 7 cells, dark blue) and adult (n = 7 cells, light blue) females (Mann–Whitney U test: W = 15, P = 0.2593). **(B)** Left, representative 3D rendering of dendritic spines from neurobiotin filled principal neurons of male pubescent and adult rats. Scale bar: 4μm. Right, dendritic spine density was similar in pubescent (n = 8 cells, dark orange) and adult (n = 8 cells, light orange) males (Mann–Whitney U test: W = 30, P = 0.8785). **(C-D)** Cumulative probability of spine lengths in female (C, blue) and male (D, orange) principal neurons. Spine lengths' distribution was significantly different between pubescent (dark) and adult (light) rats in both sexes. (Kolmogorov-Smirnov test: females, P = 0.0010; males, P = 0.0015). Insets show the average spine length: in females (C), spines were shorter in pubescent compared with adult rats, whereas in males (D), spines were longer in pubescent compared with adult rats. (Mann–Whitney U test: females, W = 4560000, P = 0.0015; males, W = 10348014, P = 0.0004). Females: pubescent, n = 2450; adult n = 3908. Males: pubescent, n = 4658; adult, n = 4639. n = spines. **(E-F)** Cumulative probability of spine head volume in female (E, blue) and male (F, orange) principal neurons. The distribution of spine length was different between pubescent (dark) and adult (light) rats in both sexes. (Kolmogorov-Smirnov test: females, P = < 0.0001; males, P = < 0.0001). Insets show the average spine head volume: in females (E), spines' heads were larger in pubescent compared with adult rats, whereas in males (F) no significant age difference in head volume was found. (Mann–Whitney U test: females, W = 4100000, P = < 0.0001; males, W = 10571080, P = 0.6047). Females: pubescent, n = 2450; adult n = 3784. Males : pubescent, n = 4640; adult, n = 4585. n = spines. **(G-H)** Cumulative probability of spine head volume in female (G, blue) and male (H, orange) principal neurons. Cumulative distribution of spine length was significantly different between pubescent (dark) and adult (light) rats in both sexes. (Kolmogorov-Smirnov test: females, P = 0.0029; males, P = 0.0345). Insets show the average spine head volume: in females (E), spine volumes were bigger in pubescent compared with adult rats, whereas in males (F) no significant age difference in spine volume was found. (Mann–Whitney U test: females, W = 4294387, P = < 0.0001; males, W = 10344742, P = 0.6020). Females: pubescent, n = 2430; adult n = 3769. Males: pubescent, n = 4586; adult, n = 4540. n = spines.

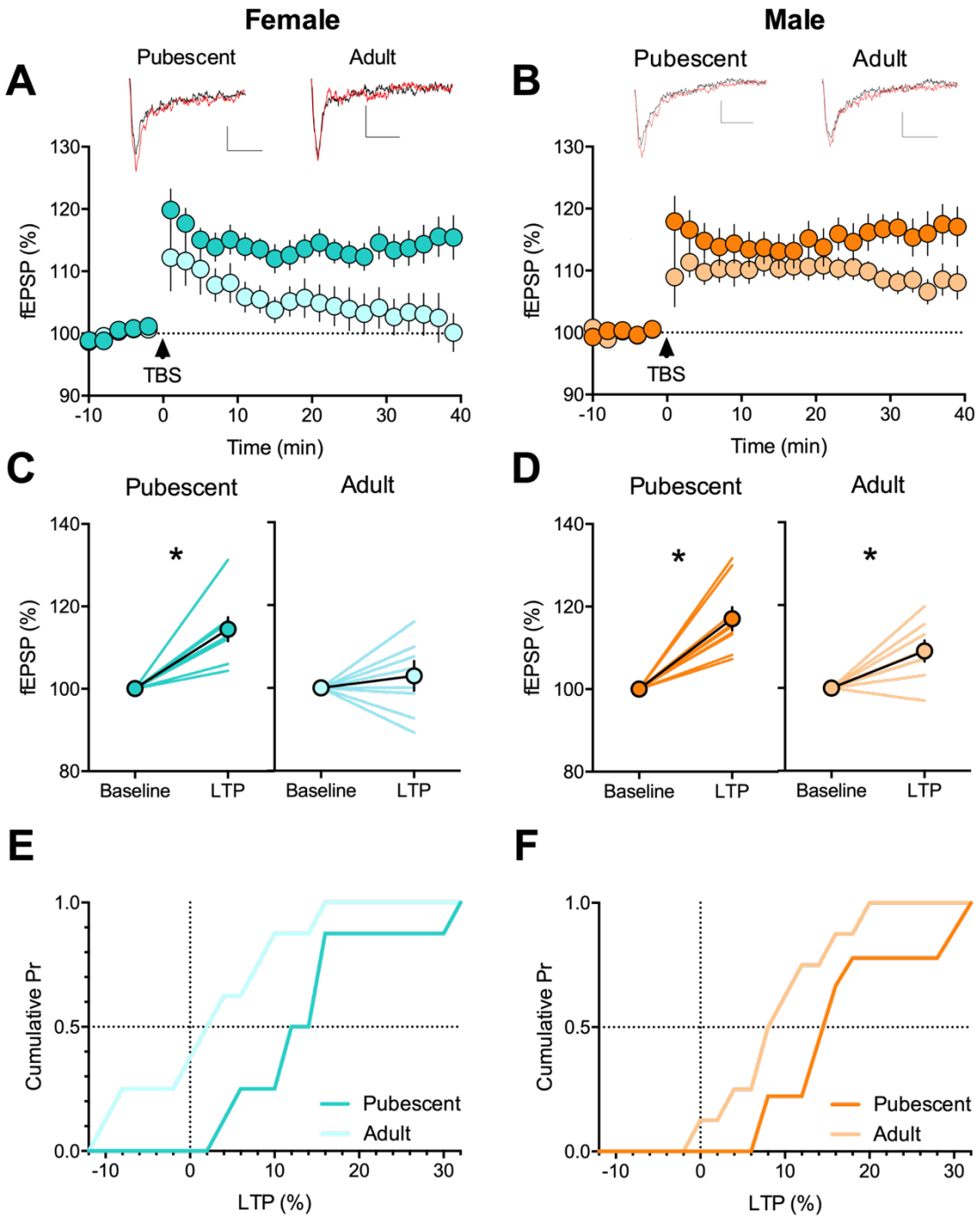
Female
Male
A
B
Pubescent
Adult
fEPSP (%)
TBS
Time (min)
C
D
Baseline
LTP
*
E
F
Cumulative Pr
LTP (%)

Figure 8: Age- and sex-dependent ablation of long-term potentiation (LTP) in the rat BLA

(**A**) Average time-courses of mean fEPSPs amplitude showing that theta-burst stimulation (TBS, indicated arrow) induced LTP at BLA synapses in pubescent females (n = 8, dark blue circles) but not in adult females (n = 8, light blue circles). Above: example traces, baseline (black) and 40 min post-stimulation (red). (**B**) In contrast, LTP was present in BLA slices obtained from both pubescent (n = 9, dark orange circles) and adult (n = 8, light orange circle) male rats. Above: example traces, baseline (black) and 40 min post-stimulation (red). (**C**) Individual experiments (simple line) and group average (circles) fEPSPs normalized amplitude before (baseline, -10 to 0 min) and after (LTP, 30-40 min) TBS showing the lack of LTP in adult females (Paired Wilcoxon test: pubescent P = 0.009, adult P = 0.547). (**D**) In contrast, LTP was induced at both pubescent and adult males BLA synapses (Paired Wilcoxon test: pubescent, P = 0.004; adult, P = 0.016). (**E-F**) Cumulative probability plot of percent LTP from individual experiments. n = individual rats, one slice per rat. All data are shown as mean ± SEM. *P<0.05. Scale bar: 0.1 mV, 10 ms.

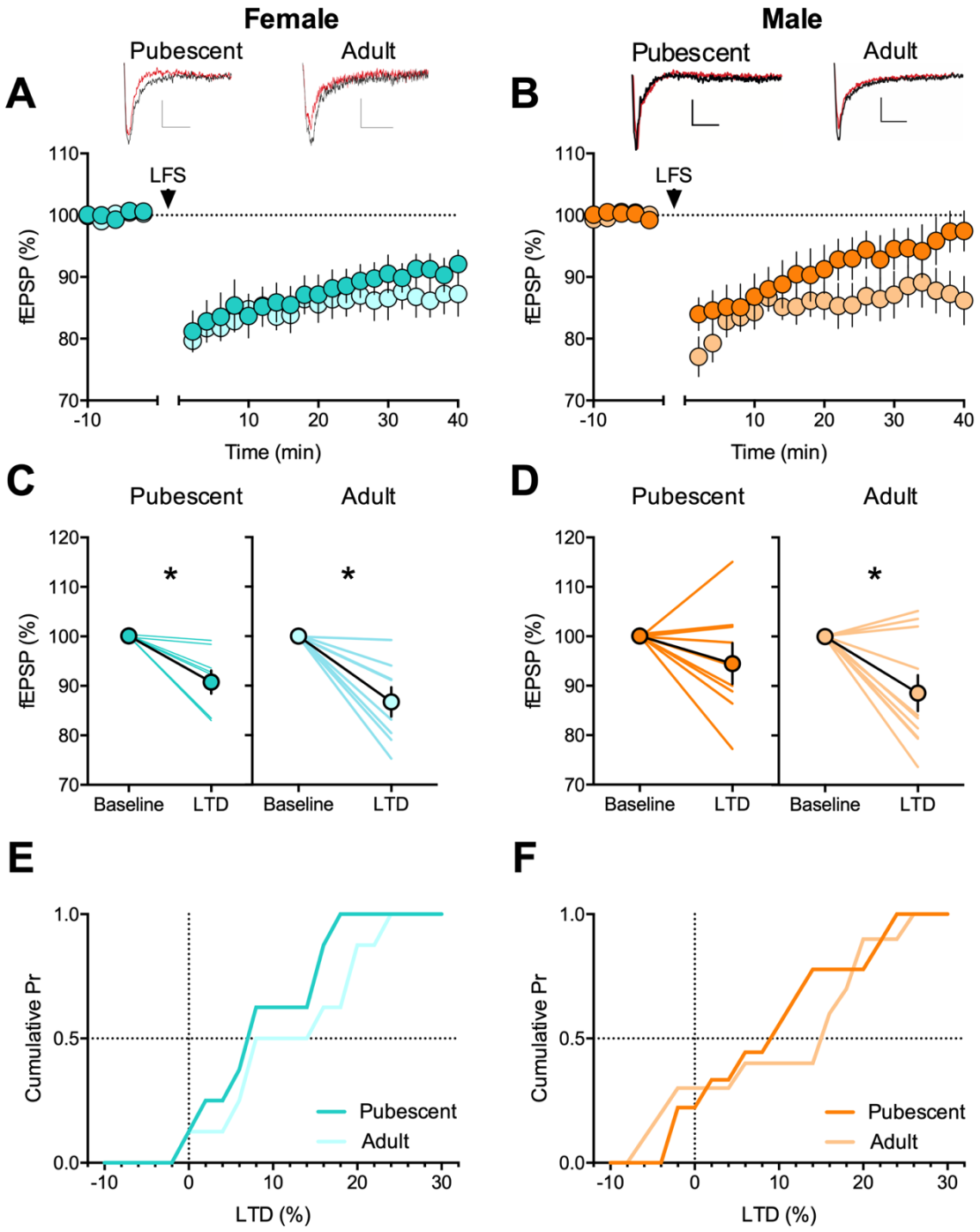
Female
Male
A
B
Pubescent
Adult
LFS
fEPSP (%)
Time (min)
C
D
Baseline
LTD
*
E
F
Cumulative Pr
LTD (%)

Figure 9: Long-term depression in the rat BLA

(**A**) Average time-courses of mean fEPSPs amplitude showing that low frequency stimulation, at 1Hz for 15 min (LFS, indicated arrow), induced LTD at BLA synapses in both pubescent (n = 7, dark blue circles) and adult (n = 8, light blue circles) females. Above: example traces, baseline (black) and 40 min post-stimulation (red). (**B**) In contrast, LTD was present in BLA slices obtained from adult (n = 10, light orange circle) but not pubescent (n = 9, dark orange circles) animals. Above: example traces, baseline (black) and 40 min post-stimulation (red). (**C**) Individual experiments (simple line) and group average (circles) fEPSPs' normalized amplitude before (baseline, -10 to 0 min) and after (LTD, 30 to 40 min) LFS showing that LTD was present at both ages in females (Paired Wilcoxon test: pubescent P = 0.016, adult P = 0.008). (**D**) In contrast, LFS failed to induce a significant LTD in pubescent male slices, whereas it induced a significant LTD in adult male slices (Paired Wilcoxon test: pubescent, P = 0.301; adult, P = 0.027). (**E-F**) Cumulative probability plot of percent LTD from individual experiments. n = individual rats, one slice per rat. All data are shown as mean ± SEM. *P<0.05. Scale bar: 0.1 mV, 10 ms.

Values are mean ± SEM.

Table 1. Intrinsic properties data by age

Measure (unit)	Condition		Value	Two-way RM ANOVA
Vm changes (mV)	**Female**	Pubescent	N=17	$F_{(interaction\ 10,\ 360)} = 0.2438$ P = 0.9915
		Adult	N=21	$F_{(age\ 1,\ 36)} = 0.7415$ P = 0.3949
	Male	Pubescent	N=22	$F_{(interaction\ 10,\ 390)} = 0.6580$ P = 0.7634
		Adult	N=19	$F_{(age\ 1,\ 39)} = 0.2693$ P = 0.6067
Number of spikes	**Female**	Pubescent	N=17	$F_{(interaction\ 16,\ 576)} = 4.595$ **P < 0.0001**
		Adult	N=21	$F_{(age\ 1,\ 36)} = 10.42$ **P = 0.0027**
	Male	Pubescent	N=22	$F_{(interaction\ 16,\ 624)} = 1.378$ P = 0.1462
		Adult	N=19	$F_{(age\ 1,\ 39)} = 1.829$ P = 0.1841
				Mann–Whitney U test
Resting membrane potential (mV)	**Female**	Pubescent	-67.96 ± 0.4775 N=17	W = 155.5 P = 0.5086
		Adult	-67.76 ± 0.4888 N=21	
	Male	Pubescent	-66.68 ± 0.6145 N=22	W = 174 P = 0.3674
		Adult	-65.86 ± 0.5777 N=19	
Rheobase (pA)	**Female**	Pubescent	164.7 ± 9.120 N=17	W = 155 P = 0.4968
		Adult	174.3 ± 7.825 N=21	
	Male	Pubescent	178.1 ± 13.66 N=21	W = 126.5 **P = 0.0476**
		Adult	141.6 ± 12.85 N=19	

Table 2. Intrinsic properties data by sex

Measure (unit)	Condition		Value	Two-way RM ANOVA
Vm changes (mV)	**Pubescent**	Female	N=17	$F_{(interaction\ 10,\ 370)} = 0.05698$ $P > 0.9999$ $F_{(sex\ 1,\ 37)} = 0.02336$ $P = 0.8794$
		Male	N=22	
	Adult	Female	N=21	$F_{(interaction\ 10,\ 380)} = 2.906$ **$P = 0.0016$** $F_{(sex\ 1,\ 38)} = 3.033$ $P = 0.0897$
		Male	N=19	
Number of spikes	**Pubescent**	Female	N=17	$F_{(interaction\ 16,\ 592)} = 0.9567$ $P = 0.5035$ $F_{(sex\ 1,\ 37)} = 0.4255$ $P = 0.5183$
		Male	N=22	
	Adult	Female	N=21	$F_{(interaction\ 16,\ 608)} = 3.535$ **$P < 0.0001$** $F_{(sex\ 1,\ 38)} = 8.291$ **$P = 0.0065$**
		Male	N=19	
				Mann–Whitney U test
Resting membrane potential (mV)	**Pubescent**	Female	-67.96 ± 0.4775 N=17	$W = 128.5$ $P = 0.0994$
		Male	-66.68 ± 0.6145 N=22	
	Adult	Female	-67.76 ± 0.4888 N=21	$W = 111$ **$P = 0.0156$**
		Male	-65.86 ± 0.5777 N=19	
Rheobase (pA)	**Pubescent**	Female	164.7 ± 9.120 N=17	$W = 150$ $P = 0.4099$
		Male	178.1 ± 13.66 N=21	
	Adult	Female	174.3 ± 7.825 N=21	$W = 112.5$ **$P = 0.0172$**
		Male	141.6 ± 12.85 N=19s	

Table 3. Action potential properties data by age

Test – Measure (unit)	Condition		Value	Mann–Whitney U test
AP threshold (mV)	**Female**	Pubescent	-39.69 ± 0.7882 N=14	W = 96 P = 0.5249
		Adult	-39.27 ± 0.8737 N=16	
	Male	Pubescent	-40.13 ± 0.4649 N=16	W = 119.5 P = 0.5631
		Adult	-40.92 ± 0.6905 N=17	
AP amplitude (mV)	**Female**	Pubescent	88.53 ± 1.907 N=14	W = 87 P = 0.3083
		Adult	85.91 ± 2.103 N=16	
	Male	Pubescent	83.06 ± 1.557 N=16	W = 92 P = 0.1181
		Adult	87.04 ± 1.954 N=17	
Half-width (ms)	**Female**	Pubescent	1.046 ± 0.03523 N=14	W = 70.5 P = 0.0857
		Adult	0.9506 ± 0.04366 N=16	
	Male	Pubescent	0.9281 ± 0.04343 N=16	W = 131 P = 0.8659
		Adult	0.9406 ± 0.05602 N=17	
Rise time (ms)	**Female**	Pubescent	0.2574 ± 0.01114 N=14	W = 76 P = 0.1389
		Adult	0.2349 ± 0.01320 N=16	
	Male	Pubescent	0.2424 ± 0.01230 N=16	W = 118 P = 0.5334
		Adult	0.2359 ± 0.01387 N=17	
Decay time (ms)	**Female**	Pubescent	0.4764 ± 0.01627 N=14	W = 65.5 P = 0.0535
		Adult	0.4207 ± 0.01898 N=16	
	Male	Pubescent	0.4039 ± 0.02374 N=16	W = 123 P = 0.6567
		Adult	0.4219 ± 0.02184 N=17	

Table 4. Action potential properties data by sex

Test – Measure (unit)	Condition		Value	Mann–Whitney U test
AP threshold (mV)	**Pubescent**	Female	-39.69 ± 0.7882 N=14	W = 107.5 P = 0.8626
		Male	-40.13 ± 0.4649 N=16	
	Adult	Female	-39.27 ± 0.8737 N=16	W = 94 P = 0.1340
		Male	-40.92 ± 0.6905 N=17	
AP amplitude (mV)	**Pubescent**	Female	88.53 ± 1.907 N=14	W = 56.5 **P = 0.0199**
		Male	83.06 ± 1.557 N=16	
	Adult	Female	85.91 ± 2.103 N=16	W = 121 P = 0.5995
		Male	87.04 ± 1.954 N=17	
Half-width (ms)	**Pubescent**	Female	1.046 ± 0.03523 N=14	W = 62 **P = 0.0371**
		Male	0.9281 ± 0.04343 N=16	
	Adult	Female	0.9506 ± 0.04366 N=16	W = 117 P = 0.6891
		Male	0.9406 ± 0.05602 N=17	
Rise time (ms)	**Pubescent**	Female	0.2574 ± 0.01114 N=14	W = 86 P = 0.2890
		Male	0.2424 ± 0.01230 N=16	
	Adult	Female	0.2349 ± 0.01320 N=16	W = 133.5 P = 0.9363
		Male	0.2359 ± 0.01387 N=17	
Decay time (ms)	**Pubescent**	Female	0.4764 ± 0.01627 N=14	W = 57 **P = 0.0218**
		Male	0.4039 ± 0.02374 N=16	
	Adult	Female	0.4207 ± 0.01898 N=16	W = 135 P = 0.9858
		Male	0.4219 ± 0.02184 N=17	

Table 5. AHP properties data by age

Test – Measure (unit)	Condition		Value	
fAHP amplitude (mV)	**Female**	Pubescent	-4.473 ± 0.5803 N=12	W = 52.50 P = 0.0685
		Adult	-5.793 ± 0.5210 N=15	
	Male	Pubescent	-7.747 ± 1.034 N=14	W = 90 P = 0.2621
		Adult	-6.142 ± 0.7349 N=17	
Time to reach fAHP (ms)	**Female**	Pubescent	0.8158 ± 0.05779 N=12	W = 89 P = 0.7577
		Adult	0.8450 ± 0.09886 N=14	
	Male	Pubescent	0.8644 ± 0.05324 N=15	W = 106 P = 0.8137
		Adult	0.7419 ± 0.05782 N=17	
mAHP amplitude (mV)	**Female**	Pubescent	-6.797 ± 0.8187 N=12	W = 34.50 **P = 0.0033**
		Adult	-10.35 ± 0.7579 N=16	
	Male	Pubescent	-7.769 ± 0.7879 N=15	W = 111.5 P = 0.5574
		Adult	-8.624 ± 0.8335 N=17	
Time to reach mAHP (ms)	**Female**	Pubescent	62.29 ± 5.277 N=12	W = 73 P = 0.3015
		Adult	69.65 ± 4.681 N=16	
	Male	Pubescent	53.29 ± 5.994 N=15	W = 97 P = 0.2613
		Adult	62.64 ± 6.326 N=17	

Table 6. AHP properties data by sex

Test – Measure (unit)	Condition		Value	
fAHP amplitude (mV)	**Pubescent**	Female	-4.473 ± 0.5803 N=12	W = 41 **P = 0.0260**
		Male	-7.747 ± 1.034 N=14	
	Adult	Female	-5.793 ± 0.5210 N=15	W = 114 P = 0.6281
		Male	-6.142 ± 0.7349 N=17	
Time to reach fAHP (ms)	**Pubescent**	Female	0.8158 ± 0.05779 N=12	W = 75 P = 0.6579
		Male	0.8450 ± 0.09886 N=14	
	Adult	Female	0.8644 ± 0.05324 N=15	W = 94.50 P = 0.2130
		Male	0.7419 ± 0.05782 N=17	
mAHP amplitude (mV)	**Pubescent**	Female	-6.797 ± 0.8187 N=12	W = 73 P = 0.4271
		Male	-7.769 ± 0.7879 N=15	
	Adult	Female	-10.35 ± 0.7579 N=16	W = 104 P = 0.2604
		Male	-8.624 ± 0.8335 N=17	
Time to reach mAHP (ms)	**Pubescent**	Female	62.29 ± 5.277 N=12	W = 60 P = 0.1523
		Male	53.29 ± 5.994 N=15	
	Adult	Female	69.65 ± 4.681 N=16	W = 100 P = 0.2039
		Male	62.64 ± 6.326 N=17	

Table 7. fEPSP input-output data by age

Measure (unit)	Condition		Value	Two-way RM ANOVA
Input:	**Female**	Pubescent	N=10	$F_{(interaction\ 14,224)} = 6.036$ **P < 0.0001**
Stimulus intensity (μA)		Adult	N=8	$F_{(input\ 14,\ 224)} = 224.2$ **P < 0.0001**
				$F_{(age\ 1,16)} = 2.694$ P = 0.1203
Output:	**Male**	Pubescent	N=8	$F_{(interaction\ 14,224)} = 5.289$ **P < 0.0001**
fEPSP amplitude (mV)		Adult	N=10	$F_{(input\ 14,\ 224)} = 183.3$ **P < 0.0001**
				$F_{(age\ 1,16)} = 4.542$ **P = 0.0489**
				Mann–Whitney U test
Maximum	**Female**	Pubescent	0.4715 ± 0.02287 N=10	W = 19 P = 0.0676
fEPSP amplitude (mV)		Adult	0.3911 ± 0.01765 N=8	
	Male	Pubescent	0.5593 ± 0.03383 N=8	W = 9.5 **P = 0.0048**
		Adult	0.4073 ± 0.03156 N=10	

Table 8. fEPSP input-output data by sex

Measure (unit)	Condition		Value	Two-way RM ANOVA
Input:	**Pubescent**	Female	N=10	$F_{(interaction\ 14,\ 224)} = 3.333$ **P < 0.0001**
Stimulus intensity (μA)		Male	N=8	$F_{(input\ 14,\ 224)} = 221.8$ **P < 0.0001**
				$F_{(sex\ 1,\ 16)} = 0.07027$ P = 0.7943
Output:	**Adult**	Female	N=8	$F_{(interaction\ 14,\ 224)} = 2.518$ **P = 0.0024**
fEPSP amplitude (mV)		Male	N=10	$F_{(input\ 14,\ 224)} = 170.7$ **P < 0.0001**
				$F_{(sex\ 1,\ 16)} = 0.459$ P = 0.5331
				Mann–Whitney U test
Maximum	**Pubescent**	Female	0.4715 ± 0.02287 N=10	W = 18.50 P = 0.0577
fEPSP amplitude (mV)		Male	0.5593 ± 0.03383 N=8	
	Adult	Female	0.3911 ± 0.01765 N=8	W = 31 P = 0.4598
		Male	0.4073 ± 0.03156 N=10	

Table 9. AMPA/NMDA ratio data by age

Test – Measure (unit)	Condition		Value	Mann–Whitney U test
AMPA/NMDA ratio	**Female**	Pubescent	0.6181 ± 0.06533 N=12	W = 35.5 P = 0.1997
		Adult	0.7712 ± 0.07989 N=9	
	Male	Pubescent	1.049 ± 0.1373 N=12	W = 45 P = 0.2115
		Adult	0.7719 ± 0.08110 N=11	

Table 10. AMPA/NMDA ratio data by sex

Test – Measure (unit)	Condition		Value	Mann–Whitney U test
AMPA/NMDA ratio	**Pubescent**	Female	0.6181 ± 0.06533 N=12	W = 32 **P = 0.0200**
		Male	1.049 ± 0.1373 N=12	
	Adult	Female	0.7712 ± 0.07989 N=9	W = 49 P > 0.9999
		Male	0.7719 ± 0.08110 N=11	

Table 11. sEPSC properties data by age

Measure (unit)	Condition		Value	Mann–Whitney U test
sEPSC frequency (Hz)	**Male**	Pubescent	4.514 ± 0.3845 N=10	W = 36 P = 0.4967
		Adult	5.001 ± 0.4688 N=9	
	Female	Pubescent	4.835 ± 0.3826 N=10	W = 45 P > 0.9999
		Adult	4.683 ± 0.4421 N=9	
sEPSC amplitude (pA)	**Male**	Pubescent	17. 46 ± 1.381 N=10	W = 40 P = 0.7197
		Adult	18.09 ± 1.511 N=9	
	Female	Pubescent	15.32 ± 0.7851 N=10	W = 12 **P = 0.0057**
		Adult	18.68 ± 0.5933 N=9	
				Two-way RM ANOVA
sEPSC amplitude distribution (pA)	**Male**	Pubescent	N=10	$F_{(interaction\ 11,\ 187)}$ = 0.09448 P > 0.9999
		Adult	N=9	$F_{(amplitude\ 11,\ 187)}$ = 61.99 **P < 0.0001**
				$F_{(age\ 1,\ 17)}$ = 0.1383 P = 0.7146
	Female	Pubescent	N=10	$F_{(interaction\ 11,\ 187)}$ = 8.741 **P < 0.0001**
		Adult	N=9	$F_{(amplitude\ 11,\ 187)}$ = 182.9 **P < 0.0001**
				$F_{(age\ 1,\ 17)}$ = 6.624 **P = 0.0197**

Table 12. sEPSC properties data by sex

Measure (unit)	Condition		Value	Mann–Whitney U test
sEPSC frequency (Hz)	**Pubescent**	Male	4.514 ± 0.3845 N=10	W = 44 P = 0.6842
		Female	4.835 ± 0.3826 N=10	
	Adult	Male	5.001 ± 0.4688 N=9	W = 37 P = 0.7962
		Female	4.683 ± 0.4421 N=9	
sEPSC amplitude (pA)	**Pubescent**	Male	17. 46 ± 1.381 N=10	W = 38 P = 0.3930
		Female	15.32 ± 0.7851 N=10	
	Adult	Male	18.09 ± 1.511 N=9	W = 26 P = 0.2224
		Female	18.68 ± 0.5933 N=9	
				Two-way RM ANOVA
sEPSC amplitude distribution (pA)	**Pubescent**	Male	N=10	$F_{(interaction\ 11,\ 198)} = 1.353$ P = 0.1978 $F_{(amplitude\ 11,\ 198)} = 94.39$ **P < 0.0001** $F_{(sex\ 1,\ 18)} = 2.362$ P = 0.1417
		Female	N=10	
	Adult	Male	N=9	$F_{(interaction\ 11,\ 176)} = 0.8472$ P = 0.5932 $F_{(amplitude\ 11,\ 176)} = 98.47$ **P < 0.0001** $F_{(sex\ 1,\ 16)} = 0.4174$ P = 0.5274
		Female	N=9	

Table 13. Dendritic spine data by sex

Measure (unit)	Condition		Value	Mann–Whitney U test
Spine density (1/10μm)	**Male**	Pubescent	17.77 ± N=8	W = 30 P = 0.8785
		Adult	17.67 ± 1.545 N=8	
	Female	Pubescent	14.83 ± 1.476 N=7	W = 15 P = 0.2593
		Adult	17.30 ± 1.236 N=7	
Spine length (μm)	**Male**	Pubescent	1.257 ± 0.01079 N=4658	W = 10348014 **P = 0.0004**
		Adult	1.206 ± 0.01067 N=4639	
	Female	Pubescent	1.261 ± 0.01514 N=2450	W = 4560000 **P = 0.0015**
		Adult	1.365 ± 0.01450 N=3908	
Spine head diameter (μm)	**Male**	Pubescent	0.3264 ± 0.001784 N=4640	W = 10571080 P = 0.6047
		Adult	0.3284 ± 0.001928 N=4585	
	Female	Pubescent	0.3472 ± 0.002399 N=2450	W = 4100000 **P = < 0.0001**
		Adult	0.3213 ± 0.001678 N=3784	
Spine volume (μm^3)	**Male**	Pubescent	0.08388 ± 0.001039 N=4586	W = 10344742 P = 0.6020
		Adult	0.08596 ± 0.001131 N=4540	
	Female	Pubescent	0.08953 ± 0.001536 N=2430	W = 4294387 **P = < 0.0001**
		Adult	0.08053 ± 0.001105 N=3769	
				Kolmogorov-Smirnov test
Spine length cumulative distribution	**Male**	Pubescent	N=4658	**P = 0.0015**
		Adult	N=4639	
	Female	Pubescent	N=2450	P = 0.0010
		Adult	N=3908	
Spine head diameter cumulative distribution	**Male**	Pubescent	N=4640	**P = < 0.0001**
		Adult	N=4585	
	Female	Pubescent	N=2450	**P = < 0.0001**
		Adult	N=3784	
Spine volume cumulative distribution	**Male**	Pubescent	N=4586	**P = 0.0345**
		Adult	N=4540	
	Female	Pubescent	N=2430	**P = 0.0029**
		Adult	N=3769	

Table 14. Dendritic spine data by age

Measure (unit)	Condition		Value	Mann–Whitney U test
Spine density (1/10μm)	**Pubescent**	Male	17.77 ± 2.517 N=8	W = 23 P = 0.6126
		Female	14.83 ± 1.476 N=7	
	Adult	Male	17.67 ± 1.545 N=8	W = 28 P > 0.9999
		Female	17.30 ± 1.236 N=7	
Spine length (μm)	**Pubescent**	Male	1.257 ± 0.01079 N=4658	W = 5661362 P = 0.7939
		Female	1.261 ± 0.01514 N=2450	
	Adult	Male	1.206 ± 0.01067 N=4639	W = 8325000 **P = < 0.0001**
		Female	1.365 ± 0.01450 N=3908	
Spine head diameter (μm)	**Pubescent**	Male	0.3264 ± 0.001784 N=4640	W = 5022000 **P = < 0.0001**
		Female	0.3472 ± 0.002399 N=2450	
	Adult	Male	0.3284 ± 0.001928 N=4585	W = 8599214 P = 0.4911
		Female	0.3213 ± 0.001678 N=3784	
Spine volume (μm^3)	**Pubescent**	Male	0.08388 ± 0.001039 N=4586	W = 5289349 **P = 0.0004**
		Female	0.08953 ± 0.001536 N=2430	
	Adult	Male	0.08596 ± 0.001131 N=4540	W = 8526396 P = 0.7878
		Female	0.08053 ± 0.001105 N=3769	
				Kolmogorov-Smirnov test
Spine length cumulative distribution	**Pubescent**	Male	N=4658	P = 0.4147
		Female	N=4639	
	Adult	Male	N=2450	**P < 0.0001**
		Female	N=3908	
Spine head diameter cumulative distribution	**Pubescent**	Male	N=4640	**P = < 0.0001**
		Female	N=2450	
	Adult	Male	N=4585	**P = < 0.0001**
		Female	N=3784	
Spine volume cumulative distribution	**Pubescent**	Male	N=4586	**P = 0.0021**
		Female	N=2430	
	Adult	Male	N=4540	**P = 0.0008**
		Female	N=3769	

Table 15. TBS-LTP data

Measure (unit)	Condition		Value	Wilcoxon signed-rank test
TBS-LTP Normalized fEPSP 0-10 min baseline (%) vs 30-40min post-tetanus (%)	**Female**	Pubescent	114.5 ± 2.915 N = 8	**P = 0.0078**
		Adult	102.4 ± 3.173 N = 8	P = 0.5469
	Male	Pubescent	117.0 ± 2.853 N = 9	**P = 0.0039**
		Adult	109.2 ± 2.565 N = 8	**P = 0.0156**

Table 16. LFS-LTD data

Measure (unit)	Condition		Value	Wilcoxon signed-rank test
LFS-LTD Normalized fEPSP 0-10 min baseline (%) vs 30-40min post-tetanus (%)	**Female**	Pubescent	91.82 ± 2.432 N = 7	**P = 0.0156**
		Adult	86.71 ± 2.968 N = 8	**P = 0.0078**
	Male	Pubescent	94.95 ± 3.676 N = 9	P = 0.3008
		Adult	88.58 ± 3.635 N = 10	**P = 0.0273**